Journal of Research of the National Bureau of Standards Vol. 46, No. 5, May 1951 Research Paper 2207

Wind Tides in Small Closed Channels

Garbis H. Keulegan

In addition to the generation of waves, a wind produces a mass transport in a body of water resulting in the lowering of the level at the windward side and rise at the leeward side, which is called wind tide or set-up. Two effects of the wind are involved: the surface traction on the water, and the form resistance of the waves. This paper presents the theoretical background of the subject and experimental results. It was discovered that formation of waves in an experimental channel could be inhibited by adding small amounts of soap or detergent to the water. This made it possible to study the surface traction effect separately. The effect was studied for both laminar and turbulent motion of the drift and gravity currents produced by the wind. The set-up computed from measured wind and water surface velocities agreed with theory. Regardless of the flow regime, the set-up was unaffected by viscosity and independent of the depth-length ratio of the channel. The additional set-up due to presence of waves could be correlated only by introducing a characteristic velocity. This additional set-up appears to vary as the square root of the depth-length ratio. The relation of the characteristic velocity to the critical velocity for wind generation is discussed. The derived empirical formula for set-up is compared with observations in Lake Erie.

I. Introduction

Early in the course of a comprehensive investigation of density currents now under way, the question arose as to what phenomena might have a probable bearing, no matter how remote, on the general problem of density currents and especially on the stability of the interface between two fluids of different densities. Among such phenomena are the disturbances that may be introduced by wind-generated surface waves on the interface between two layers of different densities such as occur in lakes and in the lower reaches of rivers emptying into the ocean.

At least two ways in which surface wind waves may affect the interface may be imagined. The first possibility is that internal waves will be generated as a response to the surface waves. This, however, is very unlikely to happen. It is well known that a two-layer system of liquids with a free surface is a system of two degrees of freedom. To one degree of freedom there corresponds the ordinary waves of a homogeneous liquid, and to the other the internal waves of the interface. The velocities of propagation of these two types of waves are unequal, and the particle motions are significantly different from each other. In ordinary waves of a homogeneous liquid, the particle motions along a given vertical line are in the same direction from the bottom to the free surface. With internal waves on the other hand, the particle motions are oppositely directed in the two layers of different densities. It follows that whatever may be the agency that causes the ordinary type of waves in a homogeneous liquid, the same agency cannot produce internal waves if the homogeneous system is replaced by a system of two layers of liquids. Wind waves are surface waves of ordinary type and therefore will not excite internal waves. If internal waves are to be created, they must be produced by displacements of the internal surface that will leave the free surface practically smooth.

The second possible effect of surface wind waves arises from their tendency to produce turbulence in the region occupied by the interface, which causes mixing of the two liquids. It is conceivable that this mixing is brought about in two ways. First, wind-generated waves are associated inherently with turbulence, and a progressive downward movement of turbulence may reach the level of the interface. If the density difference at the two sides of the interface is small, and if the turbulence fluctuations are sufficiently strong, a gradual mixing of the liquids obviously will take place.

The second and more significant way in which mixing at the interface might occur may be illustrated by the case of a lake subjected to wind wave where there is a considerable wind tide or set-up present. If there are two layers of liquids of different densities in the lake, the set-up will produce circulations of opposite directions in the two layers and thereby will cause mixing. If the density differences are small, a similar effect may also be expected to occur in the case of salt intrusion in a river when the wind is blowing in the upstream direction. The smaller the river velocity, the larger will be the mixing due to wind effects.

Before considering the effect on interfacial stability of surface disturbances caused by wind, it is necessary that sufficiently full information be obtained on the dynamical and geometrical characteristics of the wind waves and especially of wind waves in shallow and long channels. There appear to be no complete investigations, either theoretical or experimental, regarding such waves. Having in mind the excellent theoretical work of Sverdrup and Munk [1][1] on wind waves and swells originating in

[1] Figures in brackets indicate the literature references at the end of this paper

deep waters, it was thought that an experimental investigation relating to shallow waters would be a relatively simple matter. It was soon evident that there are many difficulties in the study of wind waves in a laboratory channel with shallow water that are absent in the case relating to deep water. An extensive program of investigation is practically unavoidable. As the subject is of much wider interest and practical importance than merely in its relation to density currents, a separate project was initiated. For convenience this project has been divided into three parts: (1) wind tides or set-up in small channels, (2) the dissipation characteristics of oscillatory progressive waves in long shallow channels, and (3) the growth of wind waves in height and length in long shallow channels.

The present paper deals with the first subject, that is, wind tides or set-up in small closed channels. This subject is of considerable practical importance in relation to wind effects on long shallow lakes and the feasibility of model tests. The problem of Lake Okeechobee falls into this category. Although a final solution of the question of model testing and of valid transference equations is not reached, nevertheless the results obtained represent a method of approach toward this solution.

II. Theoretical Developments

1. Generalized Surface Equation

The generalized surface equation is the differential equation involving the surface displacement of a limited body of water, the free surface being subjected to a tangential stress. We shall consider a channel closed at its ends with a constant width throughout and the bottom horizontal. The surface equation can be established very conveniently by considering the general equations of motion of the Navier type.

Selecting the origin of the axes at the bottom, with x along the channel axis and z vertical and drawn upwards as in figure 1, the equations of motion are:

$$\frac{\partial u}{\partial t}+u\frac{\partial u}{\partial x}+w\frac{\partial u}{\partial z}=-\frac{1}{\rho}\frac{\partial p}{\partial x}+\frac{1}{\rho}\left[\frac{\partial N_1}{\partial x}+\frac{\partial T_2}{\partial z}\right], \quad (1)$$

$$\frac{\partial w}{\partial t}+u\frac{\partial w}{\partial x}+w\frac{\partial w}{\partial z}=-\frac{1}{\rho}\frac{\partial p}{\partial z}-g+\frac{1}{\rho}\left[\frac{\partial T_2}{\partial x}+\frac{\partial N_3}{\partial z}\right]. \quad (2)$$

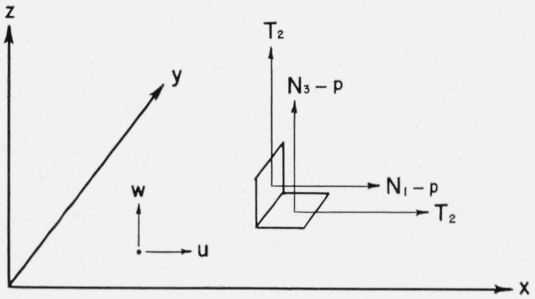

FIGURE 1. *Coordinate axes and stresses.*

Here u and w are the velocity components parallel to the x and z axes, respectively, p is the pressure, g the acceleration of gravity, and ρ the density of the liquid. The quantities N_1, N_3, T_2, are the tractional stresses as shown in figure 1. In the notation of Lamb, $N_1=p+p_{xx}$, $N_3=p+p_{zz}$, and $T_2=p_{xz}$.

The equations in the form given are too general and too difficult to integrate. In the case of a long shallow channel some simplifying assumptions may be adopted. These assumptions are commonly resorted to in solutions of boundary layer flow problems and are well known. As the surface curvature is small, the vertical acceleration and the normal traction N_3 will be neglected. As the surface displacement is small, the normal traction N_1 will be neglected. The variation of T_2 with respect to x is negligible since the channel is very long. Accordingly, the simplified forms of the equations of motion, writing τ for T_2 are

$$\frac{\partial u}{\partial t}+u\frac{\partial u}{\partial z}+w\frac{\partial u}{\partial z}=-\frac{1}{\rho}\frac{\partial p}{\partial x}+\frac{1}{\rho}\frac{\partial \tau}{\partial x}, \quad (3)$$

$$0=-\frac{1}{\rho}\frac{\partial p}{\partial z}-g. \quad (4)$$

It is to be noted that one consequence of the assumptions is to regard the pressures as hydrostatic. For the long central portion of the channel, these forms of the equations are sufficiently valid. They fail, however, to represent the conditions of flow at the ends of the channel.

Denoting the undisturbed depth of the water by H, as in figure 2, the surface displacement as measured from the initial level by h, and the atmospheric pressure by p_a, eq 4 yields

$$p=\rho g\,(H+h-z)+p_a. \quad (5)$$

Substituting in eq 3,

$$\frac{\partial u}{\partial t}+u\frac{\partial u}{\partial x}+w\frac{\partial u}{\partial z}=-g\frac{\partial h}{\partial x}-\frac{1}{\rho}\frac{\partial p_a}{\partial x}+\frac{1}{\rho}\frac{\partial \tau}{\partial z}. \quad (6)$$

Now, since the liquid is incompressible,

$$\frac{\partial u}{\partial x}+\frac{\partial w}{\partial z}=0. \quad (7)$$

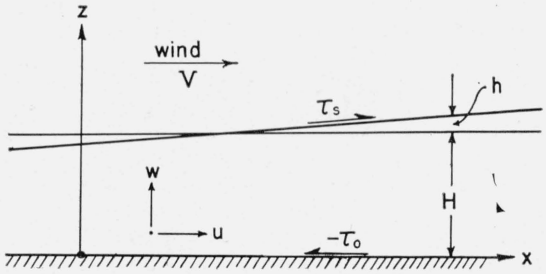

FIGURE 2. *Water levels and surface shears*

The rule

$$w\frac{\partial u}{\partial z}=\frac{\partial}{\partial z}(wu)-u\frac{\partial w}{\partial z}, \tag{8}$$

combined with eq 7 yields

$$w\frac{\partial u}{\partial z}=\frac{\partial}{\partial z}(wu)+u\frac{\partial u}{\partial x}. \tag{9}$$

Substituting this in eq 6,

$$\frac{\partial u}{\partial t}+\frac{\partial u^2}{\partial x}+\frac{\partial}{\partial z}(wu)=-g\frac{\partial h}{\partial x}-\frac{1}{\rho}\frac{\partial p_a}{\partial x}+\frac{1}{\rho}\frac{\partial \tau}{\partial z}. \tag{10}$$

Multiplying the two sides of the equation by dz, integrating with respect to z between the limits 0 and $(H+h)$, and noting that $w=0$ at the bottom where $z=0$,

$$\left.\begin{aligned}&\int_0^{H+h}\frac{\partial u}{\partial t}\,dz+\int_0^{H+h}\frac{\partial u^2}{\partial x}\,dz+w_s u_s=\\&-\left(g\frac{\partial h}{\partial x}+\frac{1}{\rho}\frac{\partial p_a}{\partial x}\right)(H+h)+\frac{1}{\rho}(\tau_s+\tau_0),\end{aligned}\right\} \tag{11}$$

where w_s and u_s are the velocity components at the free surface, τ_s and $-\tau_0$ are the tangential stresses at the free surface and at the bottom (see fig. 2). We may express w_s in terms of u_s by considering the surface kinematic condition that a particle at the free surface remains on the surface. Symbolically,

$$w_s=\frac{\partial h}{\partial t}+u_s\frac{\partial h}{\partial x},\quad z=H+h. \tag{12}$$

Introducing this in eq 11 and remembering Leibnitz's rule for differentiation under the integral sign, we have

$$\left.\begin{aligned}&\frac{\partial}{\partial t}\int_0^{H+h}u\,dz+\frac{\partial}{\partial x}\int_0^{H+h}u^2dz=\\&-\left(g\frac{\partial h}{\partial x}+\frac{1}{\rho}\frac{\partial p_a}{\partial x}\right)(H+h)+\frac{1}{\rho}(\tau_s+\tau_0).\end{aligned}\right\} \tag{13}$$

This is the generalized differential equation of the surface for a long body of water subjected to the surface tractions τ_s and $-\tau_0$. The terms on the left-hand side are the acceleration terms.

If the conditions are steady, as when the wind has acted with uniform intensity over the body of water for a long time, the equation reduces to

$$\frac{\partial}{\partial x}\int_0^{H+h}u^2dz=-\left(g\frac{\partial h}{\partial x}+\frac{1}{\rho}\frac{\partial p_a}{\partial x}\right)(H+h)+\frac{1}{\rho}(\tau_s+\tau_0). \tag{15}$$

Under certain assumptions, to be discussed later, the acceleration term on the left-hand side of the equation may be neglected. Thus, the surface equation reduces to

$$\frac{\partial h}{\partial x}+\frac{1}{\rho}\frac{\partial p_a}{\partial x}=\frac{1}{\rho}\frac{\tau_s+\tau_0}{g(H+h)}. \tag{16}$$

From this point on it will be supposed either that the atmospheric pressure or, more properly stated, the pressure on the free surface, does not vary with x; or that if it does vary, a correction is made so that h will denote the surface elevation after due account is made of the pressure effect. With this understanding, the basic simplified surface equation is

$$\frac{\partial h}{\partial x}=\frac{\tau_s+\tau_0}{\rho g(H+h)}. \tag{17}$$

A further simplification, based on assumptions relating to the relative values of τ_0 and τ_s, is needed. The flow in the channel is a combustion of a drift current at the surface and a gravity current at the bottom. The drift current is induced by the wind. The gravity current is induced by the inclination of the upper free surface, its direction being opposite to that of the drift current.

Denoting the mean velocity of the gravity current by u_0, the resistance of the channel bottom may be written as

$$\tau_0=k_0\rho u_0^2. \tag{18}$$

Similarly, if V is the wind velocity and ρ_a the density of the air, the surface traction may be expressed as

$$\tau_s=k_s\rho_a V^2. \tag{19}$$

Considering the ratio

$$\tau_0/\tau_s=\frac{k_0\rho u_0^2}{k_s\rho_a V^2}, \tag{20}$$

it is not obvious that τ_0 is negligible with respect to τ_s. The velocity u_0 may be small with respect to V, but since ρ is about one thousand times larger than ρ_a, the product ρu_0^2 may be a measurable portion of $\rho_a V^2$. Besides one must also consider the relative values of k_s and k_0, and at the moment it cannot be said that k_0 is smaller than k_s. For these reasons, it is better not to neglect τ_0 with respec to τ_s, but to incorporate it with τ_s. Writing

$$n=\frac{\tau_0}{\tau_s}+1, \tag{21}$$

eq 17 becomes

$$\frac{\partial h}{\partial x}=\frac{n\tau_s}{g\rho(H+h)}. \tag{22}$$

If a computation is made on the basis of pure viscous laminar motion, and this will be done in one of the following sections, it will be seen that $n=1.5$. The determination of n for turbulent motion requires some form of turbulent theory for the case under consideration. The value of n will then depend on the particular theory adopted. Hellström [2], after

adopting the Boussinesq theory for turbulent flow, finds that n varies between the values 1.15 and 1.80 for channels of moderate and very large depths. Temporarily we shall take $n=1.25$ for turbulent flow.

2. Surface Equation for Laminar Flow

From the viewpoint of theory it is important to consider the case of laminar flow. The chief interest, of course, rests on the fact that for this case a solution is easily available. In laboratory experiments, as will be shown later, this solution is of great value when the depths are small.

In viscous flow of the type envisaged

$$\tau=\mu\frac{\partial u}{\partial z}. \tag{23}$$

Substituting in eq 10, neglecting inertia terms, supposing the flow to be steady, the pressure over the surface uniform, and the surface displacements small with respect to the depth of water, there results

$$\frac{d^2u}{dz^2}=\frac{g}{\nu}\frac{dh}{dx}. \tag{24}$$

If the velocities are expressed in terms of the surface velocity, u_s, and the distances from the bottom in terms of the initial liquid depth, H, this equation may be made dimensionless. Thus, writing

$$\frac{u}{u_s}=\theta,\frac{z}{H}=\zeta, \tag{25}$$

and

$$\frac{gH^2}{\nu u_s}\frac{dh}{dx}=\alpha, \tag{26}$$

eq 24 becomes

$$\frac{d^2\theta}{d\zeta^2}=\alpha, \tag{27}$$

which is subject to the boundary conditions

$$\left.\begin{aligned}&\theta=0, \qquad \zeta=0,\\ &\theta=1, \qquad \zeta=1,\\ &\int_0^1\theta d\zeta=0.\end{aligned}\right\} \tag{28}$$

The first condition states that the velocity at the bottom is zero, the second that velocities are measured in terms of the surface velocity, and the third that the integrated flow in a vertical cross section vanishes.

The desired solution subject to the boundary conditions is

$$\theta=3\zeta^2-2\zeta, \tag{29}$$

and

$$\alpha=6. \tag{30}$$

Equation 29 gives the law of velocity distribution. In the horizontal plane at a distance of $H/3$ below the liquid surface the velocities vanish. All the particles above this plane move in the direction of the wind, and the particles below this plane move in the opposite direction. The former represents the drift current, and the latter the gravity current. Equation 30 gives the surface equation; for, using eq 26,

$$\frac{dh}{dx}=\frac{6\nu u_s}{gH^2}, \tag{31}$$

which relates the surface inclination to the depth of liquid, the surface velocity, and the kinematic viscosity of the liquid in the channel.

Now, from eq 23 and 25,

$$\tau=\frac{\mu u_s}{H}\frac{d\theta}{d\zeta}. \tag{32}$$

The surface shear and the shear at the bottom correspond to $\zeta=1$ and $\zeta=0$, respectively, and we have for these shears

$$\tau_s=4\frac{\mu u_s}{H}, \tag{33}$$

and

$$-\tau_0=-2\frac{\mu u_s}{H}; \tag{34}$$

that is, the surface shear is twice as large as the shear at bottom. The surface equation may be written also as

$$\frac{dh}{dx}=1.5\frac{\tau_s}{\rho gH}. \tag{35}$$

It is apparent that ignoring the bottom shear results in a 50-percent error.

III. Characteristics of the Experimental Channel

1. Apparatus

The apparatus, shown diagrammatically in figure 3, consisted of three parts: the entrance assemblage, the experimental channel, and the terminal assemblage.

The upstream blower in the entrance assemblage was driven by a constant speed motor. The air volume, and hence the air velocity in the experimental channel, was controlled by a damper at the intake end of the blower by means of which the intake area could be varied. The control of air velocities by this method was very satisfactory.

At the discharge end of the blower was a rectangular duct of the same dimensions as the blower discharge opening connected to a duct converging in plan to the width of the experimental channel. This was followed by a Venturi nozzle of constant

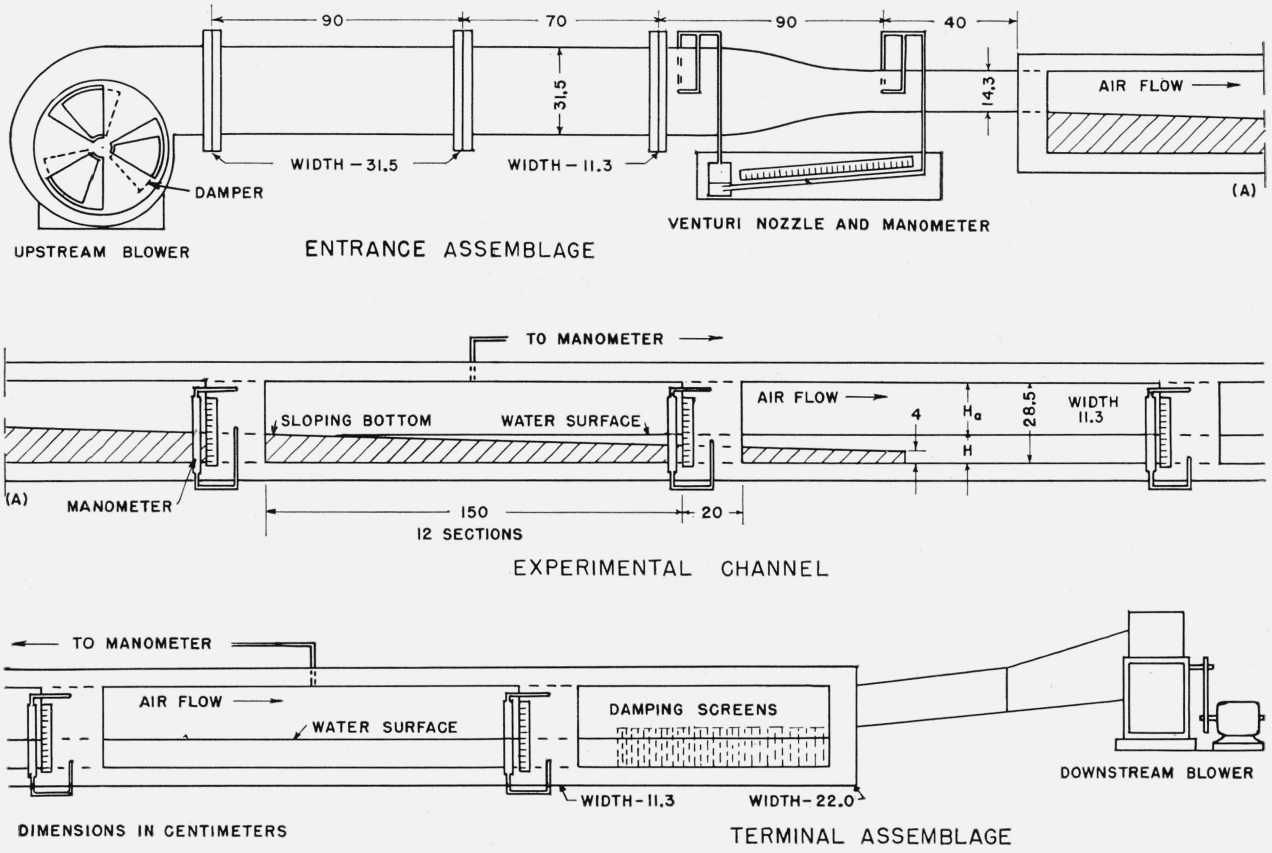

FIGURE 3. *Diagram of experimental apparatus.*

width and converging in the vertical dimension to half the height of the experimental channel. Piezometer openings in the side walls of the Venturi nozzle were connected to an inclined manometer. The Venturi was connected by a short duct to the upper half of the experimental channel. It was thought that the length of the assemblage and the lateral and vertical contractions would even out most of the irregularities in flow produced by the blower.

The experimental channel, shown in figure 3, was a closed conduit of uniform rectangular cross section, 28.5 cm deep, 11.3 cm wide, and about 20 m long. It consisted of 12 sections constructed of wood with sides of glass. The glass sections were connected by short sections made of wood. Piezometers, opening to the inside air at the top and to water at the bottom of the channel were installed in the walls of the wooden sections. The piezometer openings were connected to glass manometer wells. The average water levels in the channel were measured by the water levels in the manometers.

It was desired to make tests with different depths of water. As it was not practicable to change the elevation of the Venturi nozzle, a sloping floor was set in the upstream end of the channel. The rate of variation of the air cross section was quite small, thus assuring a nearly uniform air velocity distribution vertically.

In the top of each channel section at the center was placed a piezometer opening, and the drop in air pressure between any pair of these could be measured by connecting them to an inclined manometer. During observations of set-up, those two piezometers were used that were nearest to the ends of the fetch over which measurements were being made.

The terminal assemblage, also shown in figure 3, began at the end of the experimental channel with a section expanding in width. A succession of screens was placed at the lower end for damping of the waves. The screens were spaced about 2 cm apart initially and the spacing decreased to about ½ cm at the downstream end. The arrangement proved to be quite satisfactory. The damping was gradual and effective, there being no appreciable reflection of the waves. Downstream from this section was a duct sloping slightly upward and expanding to the size of the intake opening of the downstream blower. This blower was used in addition to the upstream one whenever high air velocities were required.

2. Calibration of the Venturi Nozzle

The mean velocity of the air stream over the water in the channel was chosen as the significant velocity to be associated with the growth of waves or with the development of wind set-up. The depth

of the channel being small, the height of the air passage over the water decreased continually in the leeward direction because of the set-up and of the increase in wave heights. Therefor it was not very practical to measure the local mean air velocity at any chosen cross section. Instead, the air velocity was deduced from the velocity at the discharge end of the Venturi nozzle. Thus if V_1 is the velocity and A_1 the area of the nozzle exit, and V is the mean air velocity in the channel for an air passage of cross-sectional area A, then $V=V_1A_1/A$. The area, A, represents the mean value of the area averaged along the entire length of the channel. Obviously, A is also the area of the air passage cross section when the water in the channel is not disturbed. In the measurements of set-up, however, the decrease of the cross section of the air passage with distance was considerable, and hence corrections were devised, as will be explained later, to obtain the value of the effective wind velocities.

The differential head reading of the inclined manometer was an indication of the velocity at the discharge end of the Venturi nozzle. The calibration was made in the following manner. The terminal assemblage at the lower end of the experimental channel was removed, and the velocities at the end section of the channel were measured. These were associated with the simultaneous readings of the Venturi manometer. The velocities at the channel end were measured by two instruments. One was a propeller-type anemometer of current manufacture that was calibrated in a wind tunnel by the Aerodynamics Section of the National Bureau of Standards. The second instrument was a small Ott current meter. Although this instrument is used ordinarily for flowing water and the calibration is likewise made in water, it can, nevertheless, be used for flowing air provided the calibration of the instrument is expressed in the form

$$N/U=f(U\sqrt{\rho}), \tag{36}$$

where N is the number of revolutions per second corresponding to the velocity, U. [3] To be sure that this relationship applied to the Ott meter to be used, it was calibrated both in water and in air. In the range where the calibration results with air and with water overlapped, the results fell on the same curve.

The Ott meter, being the smaller of the two, was set in six different positions in the channel cross section. The other instrument was set in three positions on the vertical center line. The average of the mean velocities determined in these two ways was taken to be the mean velocity of the air stream at the end cross section of the channel. Comparing the cross-sectional areas, the velocity at the nozzle was obtained in relation to the manometer reading. Following this, a second calibration was obtained after attaching to the end of the main channel an additional closed rectangular conduit of a larger cross section. In the second channel both instruments were set in six different positions.

It was gratifying to note that the Venturi nozzle velocities as observed during the calibrations could be very well represented by the theoretical expression.

$$2\rho g\Delta h=\rho_a V_1^2\left[1-\left(\frac{A_1}{A_2}\right)^2\right], \tag{37}$$

where Δh is the reading of the inclined manometer in feet of water, and A_2 is the area at the entrance of the nozzle. The final calibration chart was made by using the above formula and taking $\rho_a/\rho=1.16\times10^{-3}$, a value corresponding to an atmospheric pressure of 740 mm Hg and an air temperature of 23° C.

3. Air Velocity Distribution in Channel

In studies of the growth of waves with distance and of the development of wind set-up under natural conditions the proper selection of the elevations for the measurement of wind velocities is a difficult matter. If one could assign an operative roughness length, k, independent of the dimensions of waves excited by the wind, it would be sufficient to measure the wind velocity at a constant elevation, z_a, independent of the wind velocity. The investigations of Roll [4] concerning the wind field over the seas show that an operative constant roughness in the above sense does not exist and the roughness is dependent on the wind velocity. This naturally introduces a complication if results of investigations in the open seas are to be compared with results obtained under laboratory conditions.

Because of the limited channel dimensions there is little latitude in selecting the location for the wind velocity measurements in laboratory tests. The velocity of the wind may be taken either as the velocity at the center of the area above the water or as the mean velocity all over the area. In the present investigation the second choice was preferred. This procedure would be free of any objection provided the air velocity distributions in the channel remain always affine to each other for varying velocities and varying water depths. This matter was examined for a water surface free of waves.

One additional point that needed examination was the assumed effectiveness of the expansion caused by the sloping bottom at the entrance of the main channel (see fig. 3) in establishing uniform air velocities at the leeward end of the expansion. For this purpose two sections were chosen, one at the windward end and the other at the leeward end of the channel, and vertical air velocity traverses were made along the vertical median plane. One group of such determinations is shown in figure 4, where V represents the velocity at a distance, z_a, from the water surface, V_m the average velocity along the vertical, and H_a the height of the air gap. In this case the water depth was 4.0 cm, the air space height 24.5 cm, and the average velocity along the vertical 1,008 cm/sec. The velocity distributions at the two ends of the experimental channel are practically alike. For the same air

space similar determinations were carried out for two other velocities, namely 700 and 480 cm/sec, with results very similar to those shown in figure 4. The measurements were repeated for other air gaps, namely H_a=20.5, 17.5, 14.0 cm, with three air velocities not greatly different from those mentioned above. It was noted in every case, regardless of the air space or the magnitude of the mean air velocity, that the median vertical velocity distributions were alike in the extreme end cross sections. Thus for the comparison of the velocity distributions in each air space it should suffice to consider the averages from the measurements with a chosen air space. Such mean values are shown in figure 5. From the curve drawn in the figure we make two deductions. First, central wind velocities are about 1.1 times as large as the mean air velocity. Second, there are no large differences between the air velocities near the rigid top of the channel and those near the water surface. If anything, the air velocities near the water surface are slightly higher, as might be expected.

Next, the horizontal velocity distribution close to the water surface was examined. The results of a few traverses are shown in figure 6. The plotting is V/V_{max} versus y/B, where V_{max} is the velocity at the median plane, V the velocity at a distance, y, from one of the vertical walls, and B the width of the channel. The liquid in the channel was of large viscosity so that for large air velocities the surface would be free of waves. Three series of traverses were obtained for the surface of the liquid thus unmodified by waves corresponding to settings of the pitot tube at successive elevations, z_a, of 0.4, 0.9, and 1.7 cm above the water surface. The results are shown in the figure by the open symbols. Only one measurement of velocities was made with the liquid surface covered with waves. In these measurements the pitot tube aperture was almost at the level of the crests of the waves. The data for these tests are shown by black circles. It is important to note that for the lateral traverses the distributions of the velocities are more uniform than in the vertical traverses. The presence of the waves hardly modifies this comparison.

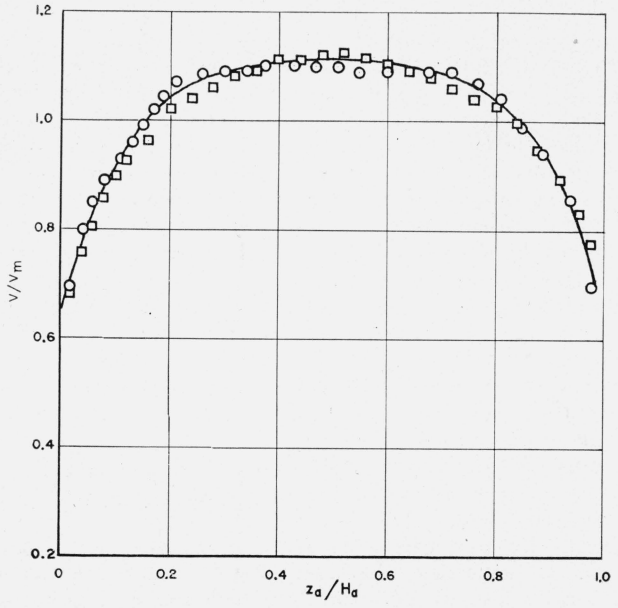

FIGURE 4. *Vertical distributions of air velocities at the ends of the channel.*

Circles, velocities at windward end; squares, velocities at leeward end.

IV. Wind Set-Up in the Absence of Waves

1. Effect of Soapy Waters on the Start of Waves

It was discovered accidentally during the conduct of the routine experiments that the addition of soap to the water inhibited the formation of waves by wind action. Ordinarily when the water in the channel was free of foreign matter, a wind with velocity of 300 to 400 cm/sec caused waves to be formed. An increase in the wind velocity above this value increased the height and length of the waves. On the other hand, when soap was introduced in the water and the wind velocity was increased gradually from zero value, it was found that no matter how great the wind velocity, the surface of the liquid resisted the formation of waves. Even at a wind velocity of 1,200 cm/sec, which was the limiting capacity of the apparatus, the soapy liquid surface was free of waves. This peculiar phenomenon could be repeated for all depths of liquid from 4 to 14.5 cm. The same condition could also be reproduced by introducing a detergent of the type sold for cleansing kitchen utensils, instead of soap.

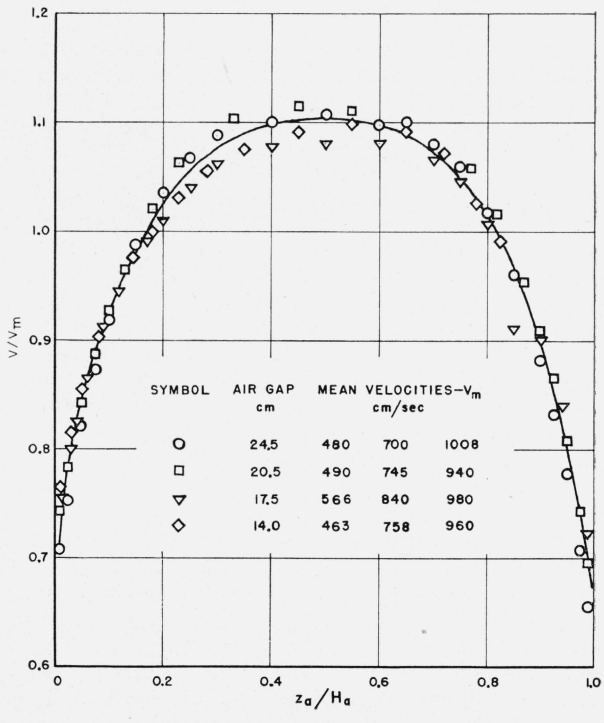

FIGURE 5. *Vertical distributions of air velocities at center-line of channel.*

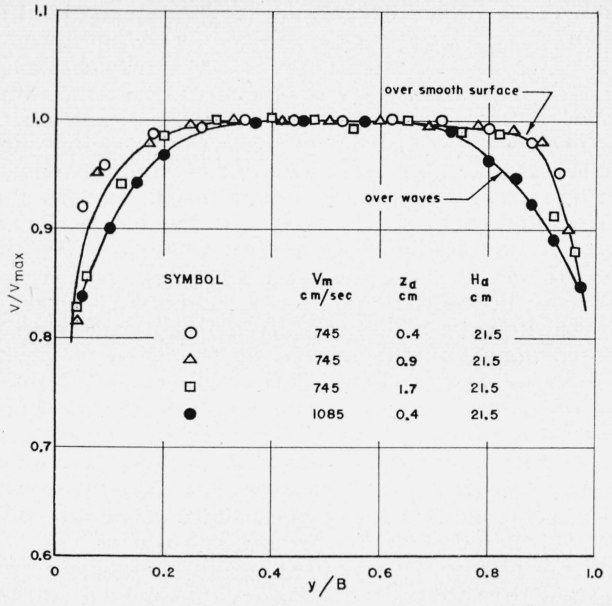

FIGURE 6. *Horizontal distributions of air velocities near liquid surface.*

It must not be inferred from the above that in contaminated waters of the kind described all wave motions are impossible. If, by a special manipulation, waves of substantial dimensions are once produced, these continue to grow in size and multiply in number after traveling long distances under the action of the wind. We have had a very significant experience demonstrating this fact which deserves a brief mention here.

The soapy water in the channel was about 10 or 11 cm deep, the two blowers were in action and, owing to the large air velocity, the water surface was considerably inclined, the greater depth, of course, being at the leeward end of the channel. The surface was smooth and free of waves. The windward edge of the water was located on the solid sloping surface at the channel entrance. To see what effect a sudden reduction of the air velocity would produce, one of the blowers was stopped quickly. Immediately a surge from the leeward end of the channel started to travel toward the windward end. At the instant that the surge reached the windward end and the water commenced to pile up on the sloping surface there, the idle blower was started again. Under the impact of the increasing wind two joining intumescenses were seen to develop at the windward water edge which moved in the leeward direction. In the movement the number of the waves continually increased and the crests became higher. Thus a limited line of waves, so to speak, was moving downstream, the length of the line increasing continually. Waves in the front of the line would be pressing forward, while at the rear new waves appeared. Finally, a long line of waves was filling the last quarter of the channel whereas the water in the rest of the channel was smooth and undisturbed. This line of waves would be seen to enter the wave dampers, and after a while the last wave of the line would be lost. Following this a new surge started moving toward the windward end. The cause of the surge was the sudden decrease of the wave friction concommitant with the disappearance of the waves. The surge reaching the windward end of the channel, a new pair of waves was seen to be formed and the entire process of wave group motion described above was repeated. The phenomenon appeared to reproduce itself periodically and uniformly. Obviously, here was a special case involving the principle of group waves and their generation under the action of wind forces. It is regrettable that, due to the pressure of the main problems of the investigation, additional time could not be devoted to the study of this unusual phenomenon.

Thus the inhibitive action of the soapy water or water containing detergent is to be associated with water surfaces initially undisturbed and therefore free of local elevations occurring over short lengths. Under these conditions, no matter how strong the wind may be, the action of the flowing air fails to start those tremors of the water surface that are always present when the water is pure and the formation of waves is impending. The action of the contaminated water cannot be explained. It would appear that neither viscosity nor surface tension have a bearing on the subject.

Once the fact became known that it was possible to operate with a smooth surface in the channel within the full capacity of the blowers even though the wind velocities were large, by merely adding soap or detergent to the water, it was decided to make full use of it. Numerous experiments were carried out under these conditions that are considered in the subsequent sections. It was felt at the time and also verified later that through these experiments a better understanding of the main problems of the investigation would result.

2. Formulation of Wind Set-Up for Smooth Water Surfaces

The term "set-up" may be defined to represent either the displacement of the water surface at the leeward end of the channel with respect to the undisturbed level of the water or the difference of the displacements of the water levels at the windward and the leeward ends of the channel, that at the windward end being negative. The displacements referred to are the values that remain after correcting for the fall of the air pressure in the channel. In this investigation the term will be used in the second sense. Thus denoting the windward and leeward displacements by h_1 and h_2, respectively, the set-up, S, is

$$S=h_2-h_1. \tag{38}$$

Observations of the set-up were made for depths of 14.5, 11, 8, 6, and 4 cm with smooth water surfaces. In every observation of the set-up for a given wind velocity the following quantities were observed. First, the reading of the Venturi nozzle manometer,

which gave the average wind velocity in the channel, was noted. Second, the elevations of the water levels in the two extreme manometer wells were observed, the distance between the wells being the nearest possible to the fetch, that is, the length of the water surface acted on by the wind. The diameters of the manometer glass tubes being 2 cm, the meniscii were hardly affected by surface tension. The meniscus positions were read by a telescope against a centimeter scale with millimeter divisions, which was placed near and parallel to the tubes. The elevations could be estimated with an accuracy of ± 0.1 mm. Third, the pressure fall in the channel air passage corresponding to the fetch was noted. This was done by connecting the extreme piezometer openings in the top of the channel to an inclined manometer, the pressure differences being read in heads of water.

Because of the inclined solid bottom at the channel entrance the fetch varied with the depth of water. The manometer well distances, L', approximating the fetches were: $L'=2{,}000$ cm for $H=14.5$ cm; $L'=1{,}850$ cm for $H=11$ and 10 cm; and $L'=1{,}725$ cm for $H=6$ and 4 cm. The set-up values observed with these lengths were reduced, after correcting for the pressure fall in the air space, to a common fetch of $L=1{,}900$ cm. As the curve of the surface displacements to a first approximation is linear, the reduction to a standard fetch is a matter of direct proportionality. That is, if S' is the set-up corresponding to L', and if the difference $L'-L$ is a small part of L, then

$$S=S'L/L'. \tag{39}$$

The results of the set-up observations, determined in this manner, for various depths of water are shown in figure 7. The set-ups observed with smooth surfaces will be denoted as S_1. In the figure S_1, expressed in centimeters, is plotted against V^2, the square of the average wind velocity, where V is expressed in centimeters per second. For a given depth of water and for a given fetch the set-up is proportional to the square of the wind velocity. From the data of figure 7 the values of S_1 for the different depths at a common wind velocity $V=1{,}000$ can be obtained. These are shown in figure 8. It is seen that the distribution of the data points is nearly linear, and the straight line drawn through the points has a slope of one to one. The interpretation, therefore, is that for a constant wind velocity and for a constant fetch the set-up is inversely proportional to the depth of water. Expressed mathematically,

$$S_1 \sim V^2/H. \tag{40}$$

Rendering the relation dimensionally correct we have, since the quantities g and L were constant in the tests,

$$\frac{S_1}{L}=A\frac{V^2}{gH}, \tag{41}$$

where A is a numerical constant having the value

$$A=3.30\times 10^{-6}. \tag{42}$$

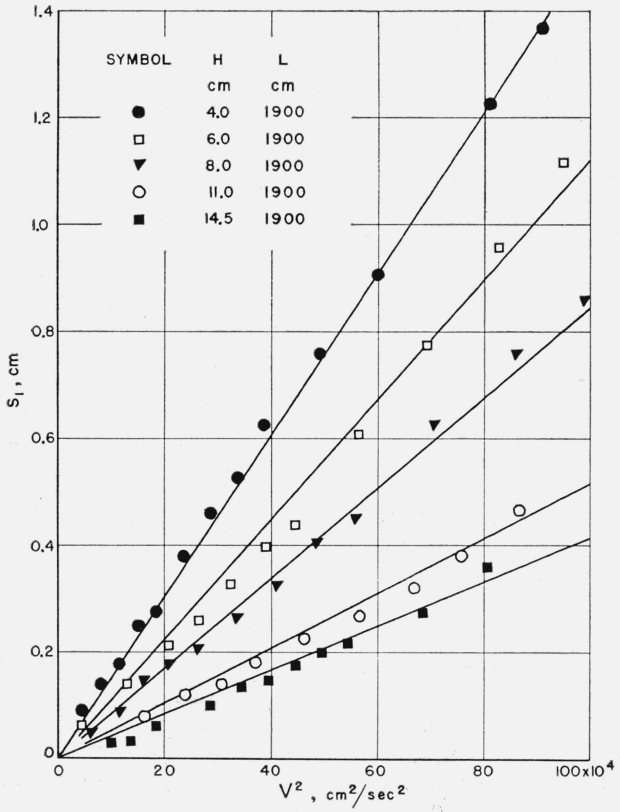

FIGURE 7. *Wind set-up in the absence of waves.*

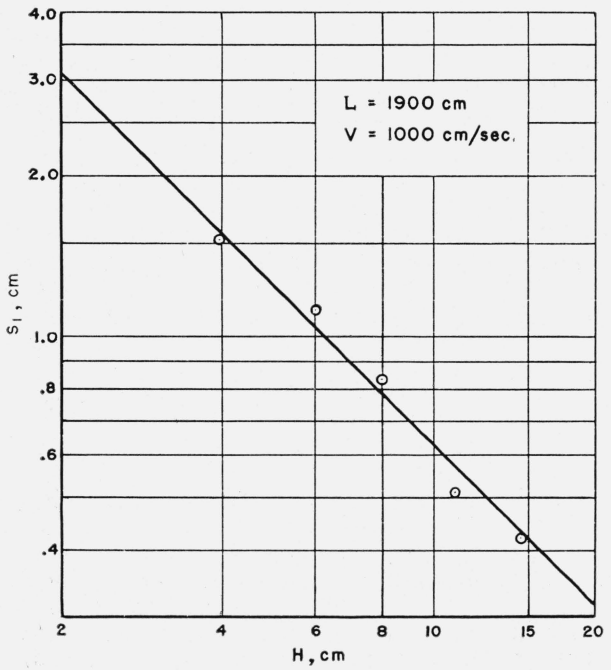

FIGURE 8. *Variation of set-up with depth in the absence of waves.*

These relations give the law of wind set-up where the wind is not of sufficient strength to excite waves and therefore the water surface is smooth.

3. Relation of Water Surface Velocities to Wind Velocities

The argument regarding the development of the final formula of the preceding section is not complete. It remains to see whether the coefficient, A, of the wind velocity term is in every respect a numerical constant unaffected by the viscosity of the liquid. This aspect of the problem will be investigated later. For the present the inquiry will be facilitated by first establishing the relationship between the surface velocities of the water and the wind velocities.

An effort was made continually during the tests to measure the water surface velocity to see whether a relationship existed between this and the air velocity, as affected by the depth of liquid and the viscosity of liquid. It was also thought desirable to see if the relationship was modified by the fact that the liquid surface was smooth or covered by waves. The change in the viscosities was brought about invariably by using sugar solutions of various concentrations.

To obtain the surface velocities, small paraffin particles were dropped from a perforation in the channel roof, and the movement of the particles along a given distance was timed by a stop watch. At the commencement of such observations, the velocities were measured over successive intervals covering the entire channel from the beginning to the end. It was found during numerous tests of this type that the surface velocities did not change with distance when the liquid depth was large and the viscosity of the liquid small. Only when the depths were small and the liquid viscosities large would the surface velocities vary with distance. Thus in the later experiments the surface velocity was measured over small lengths.

The velocity values for a given wind velocity were based on the average value of three to five individual determinations. Usually the floating particles did not maintain a constant distance from the wall during their travel. The meander of the particles, however, was such that it could be taken to be equivalent to the motion of a hypothetical particle keeping a constant midway position between the channel axis and the glass wall. A study of the lateral distribution of the surface velocities did show, and the evidence will be reproduced later in this section, that the motions of such particles give very nearly the average value of the surface velocities taken in the lateral distribution.

Representing the average surface velocity by u_s, the question to be examined is the dependence of u_s on the wind velocity V, on the liquid depth H, and on the kinematic viscosity ν of the liquid. Obviously, the relationship is of the type

$$\frac{u_s}{V}=f\left(\frac{u_s H}{\nu}\right). \tag{43}$$

For the establishment of the relationship the measurements obtained with water depths of 4, 6, 8, 11, and 14.5 cm were first considered. In some of the tests the water was charged with soap or with detergent. These observations, however, did not yield Reynolds numbers of sufficiently low values. To supplement the data other observations were undertaken with liquid depths of 8, 4, and 2 cm, using heavy sugar solutions.

The data accumulated from these extensive tests yielded the values of the parameters u_s/V and $u_s H/\nu$, which are plotted in figure 9. Obviously, when the Reynolds number is small, the viscosity of the liquid has a very marked effect on the surface velocity. In the logarithmic plotting the distribution of the points of observation for low Reynolds numbers is linear, and the line drawn has the slope one in two. Accordingly the law for the surface velocities when the Reynolds number is small is

$$\frac{u_s}{V}=K\left(\frac{u_s H}{\nu}\right)^{1/2}, \tag{44}$$

where the coefficient K is a pure number having the value

$$K=7.6\times 10^{-4}. \tag{45}$$

Starting with a Reynolds number of approximately 1,000 the ratio of the two velocities tends slowly to a constant value indicating that above this value the effect of kinematic viscosity is very slight.

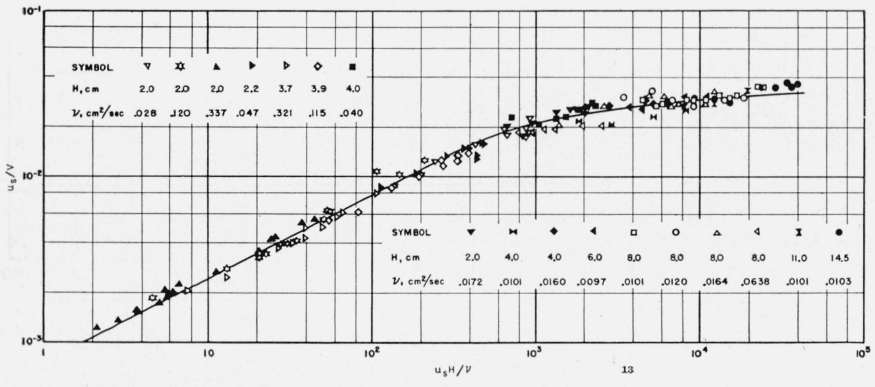

FIGURE 9. *Variation of water-surface velocities with Reynolds Number.*

Judging from the curve drawn in the figure the limiting value of the ratio is

$$\frac{u_s}{V}=0.033. \tag{46}$$

In establishing the part of the graph above a Reynolds number of 1000, test data were used without regard to the condition of the liquid surface that happened to prevail. That is, some of the data are from runs where the surface was covered with waves and other data are from runs where the surface was smooth. Where waves were present, the surface velocities used were mean values from the crests and from the troughs. Due to the close grouping of points the inference is that the surface velocities are not affected by the presence of the waves. This surely was an unexpected result, and due to its importance the question was further investigated in two additional series of experiments. In one of the series the water of the channel was treated with detergent. During the measurement of the surface velocities the surfaces were smooth and calm. The data from this series of tests are shown in figure 10. For the second series the channel water was clean, and the observations were made with air velocities yielding substantial wave formations. The data from the latter series are shown in figure 11. In the figure are drawn two straight lines; the broken line represents the average values from the tests with water surface remaining calm; the continuous line represents the average values of the individual data shown in the figure. The disparity between the two curves is less than the scatter of the individual observations, and it may be stated on this basis that the presence of waves does not appreciably affect the relation between the surface velocities and the wind velocities.

In the above discussion, the ratio of the two velocities is treated as a function of the Reynolds number based on the surface velocities. It is equally feasible to take the Reynolds number based on wind velocities. This is especially useful for comparison with prototype data. The data for this case are given in figure 12. Accordingly for Reynolds numbers below 30,000 the ratio u_s/V varies inversely with Reynolds number; for higher Reynolds numbers the ratio tends to a constant value of 0.033, roughly.

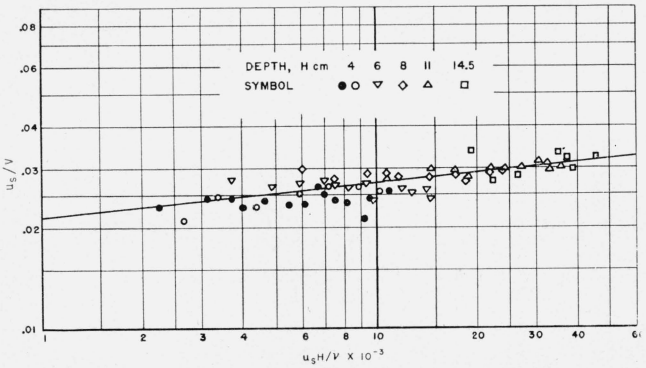

FIGURE 10. *Water-surface velocities for large wind velocities in the absence of waves.*

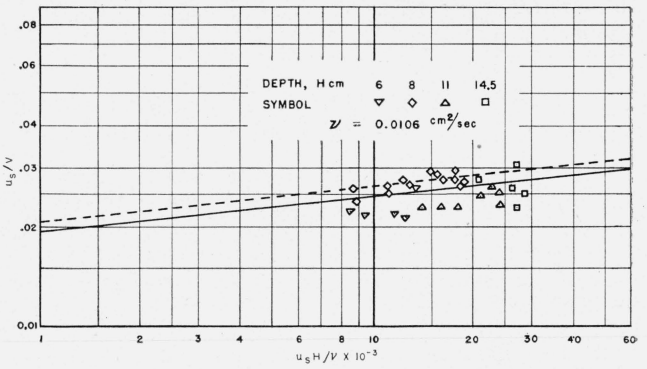

FIGURE 11. *Water-surface velocities for large wind velocities in the presence of waves.*

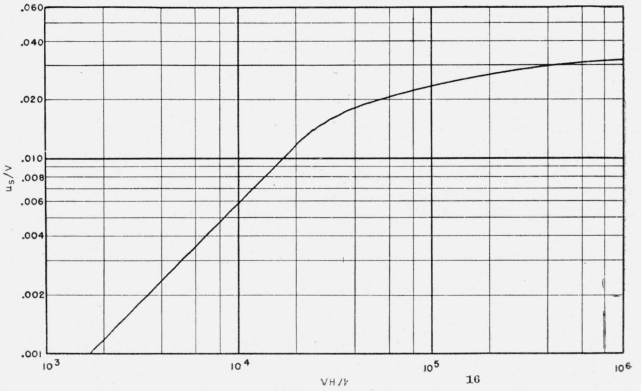

FIGURE 12. *Variation of water-surface velocities with Reynolds Number based on wind velocities.*

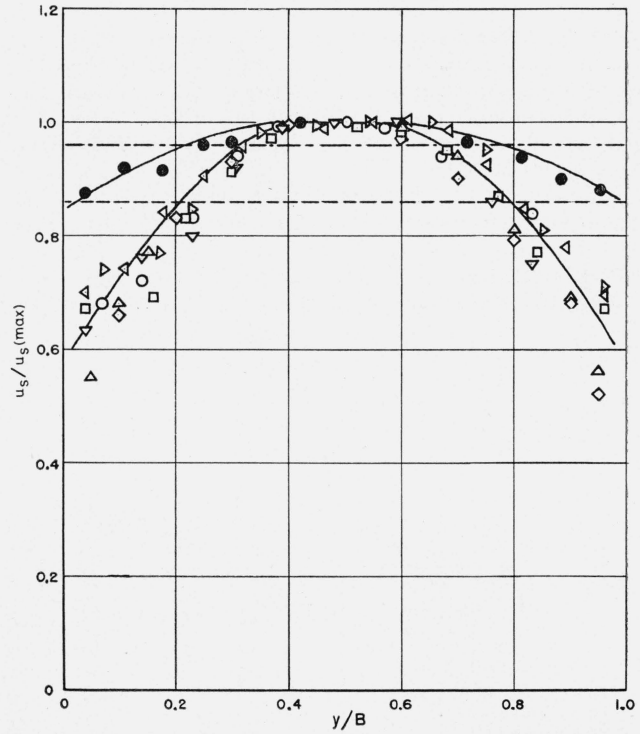

FIGURE 13. *Lateral distribution of water-surface velocities.*

Before closing the matter of the present section, the evidence that the measured surface velocities equal the averages taken across the width of the channel must be shown. The establishment of the lateral distribution of the surface velocities proved to be a very difficult task. Much time was spent and the observations were repeated many times until some assurance about the results was obtained, working always with statistical averages. Without attempting a description of the methods used, the final results are shown in the form of graphs in figure 13. The lower group of points represents test data for the case where the liquid surface was smooth and free of waves. The data points are differently indicated and correspond to liquid depths varying from 2 to 8 cm and to velocities varying from 350 to 700 cm/sec. As the points group so closely among themselves for a given distance from the walls, it did not seem necessary to indicate the velocities and the depths corresponding to specific symbols. The broken line gives the coordinate coinciding with the average velocity. According to these results a particle on the water surface at a distance of 2.2 cm from the nearest wall moves with a velocity equal to the average of the velocities in the lateral traverse. The upper group of points in the figure was obtained for a liquid surface covered with waves. The number of observations was as large as for the points below; the observations being made with various depths and with various wind velocities. In order not to confuse the appearance of the graph, only averaged values are shown since no systematic variations could be discerned in the data with respect to depth of liquid or to wind velocity. It appears as though the surface velocities vary less in a lateral traverse when waves are present. In this case also the surface velocity at a distance of about 2.2 cm away from the nearest wall represents practically the average velocity of a lateral traverse.

4. General Law of the Surface Gradient in the Absence of Waves

The regularity seen in the relationship of the surface velocities with the Reynolds numbers based either on the surface velocities or on the wind velocities suggests that perhaps a similar relationship should exist for the surface gradient.

It was remarked in the theoretical analysis of purely viscous conditions that the surface gradient may be expressed as

$$\frac{dh}{dx}=\frac{6\nu u_s}{gH^2}. \tag{31a}$$

This might be generalized to include the case of turbulent flow by writing

$$\frac{dh}{dx}=\phi_s\frac{u_s^2}{gH}, \tag{47}$$

where

$$\phi_s=\phi_s\left(\frac{u_sH}{\nu}\right). \tag{48}$$

The quantity ϕ_s may be referred to as the surface coefficient. Accordingly, the surface coefficient for the case of purely viscous flow is

$$\phi_s=6\Big/\frac{u_sH}{\nu}. \tag{49}$$

The set-up observations that were made with water

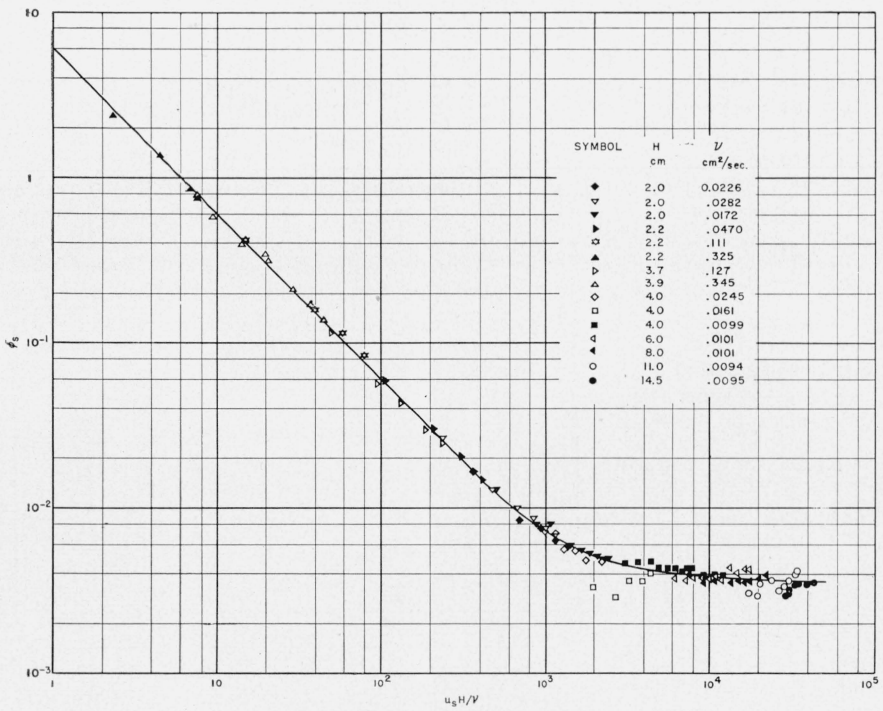

FIGURE 14. *Coefficient of surface slope in the absence of waves as a function of Reynolds Number.*

charged with soap or detergent may be used for evaluating ϕ_s corresponding to large Reynolds numbers, for in this case the surface gradient can be written also as

$$\frac{dh}{dx}=\frac{S_1}{L}. \tag{50}$$

The relation between the wind velocities and the surface velocities is given by the graph in figure 12. As regards ϕ_s for small Reynolds numbers, set-up observations were made with small depths (2 and 4 cm) and with sugar solutions of various concentrations. In these latter tests, owing to the large viscosities of the solutions, waves could be excited only with winds of large velocities and therefore there was a range of velocities that left the liquid surface calm and smooth. As an illustration, the set-up observations made with a liquid of kinematic viscosity $\nu=0.111$, a water depth $H=2.0$ cm, and a fetch $L=1{,}760$ cm, are shown in figure 18.

The determination of the surface gradient coefficient as a function of the Reynolds number is shown in figure 14. It is apparent for low Reynolds numbers, that if the coefficient be defined as in eq 47, its value is affected very markedly by the Reynolds number. The distribution of the data points is sufficiently linear to allow the drawing of a straight line through them. The line actually drawn conforms to the theoretical expression given by eq 49, and since the line represents the positions of the observed points quite accurately the theory is verified satisfactorily. There was another deduction of the theory that appeared from limited observations to be verified. According to eq 29 the particle velocity is zero at a point two-thirds of the total depth measured from the bottom. Observations of small particles that had accumulated in the channel for one reason or another indicated this deduction to be substantially true.

For high Reynolds numbers, as may be observed from the data of figure 14, the effect of Reynolds number is small and the coefficient tends to a constant value. The deduction from the data presented is that the surface velocities define completely the regime of flow in the liquid below, the flow assuming either the character of a viscous flow or a turbulent flow. The passage from one type of flow to the other type does not show the sharp and sudden transition ordinarily seen in fluid motion phenomena.

For practical applications it is desired to define the coefficient of the surface gradient in terms of the wind velocities instead of the liquid surface velocities. In this new representation

$$\frac{dh}{dx}=\phi_a\frac{V^2}{gH}, \tag{51}$$

and

$$\phi_a=\phi_a\left(\frac{VH}{\nu}\right), \tag{52}$$

where ϕ_a is the coefficient of the surface gradient in relation to wind velocity. The transfer from ϕ_s to ϕ_a is readily made by using the data in figures 9 and 14. The determinations of ϕ_a thus made are shown in figure 15. The surface gradient coefficient ϕ_a is independent of the Reynolds number VH/ν. Specifically

$$\frac{dh}{dx}=3.35\times10^{-6}\frac{V^2}{gH}. \tag{53}$$

This value of $\phi_a=3.35\times10^{-6}$ is to be compared with the value of $A=3.30\times10^{-6}$ appearing in eq 42. This then completes the argument that the coefficient, A, appearing in eq 41 is actually a numerical constant and in particular is independent of liquid viscosity.

The result shown above is one of remarkable simplicity. In terms of the shear acting on the water surface, the gradient is

$$\frac{dh}{dx}=\frac{n\tau_s}{\rho gH}, \tag{22a}$$

and comparison with eq 53, using the average value of ϕ_a from eq 42 and eq 53 yields,

$$n\tau_s=3.32\times10^{-6}\rho V^2, \tag{54}$$

where ρ is the density of the liquid. Replacing ρ with the moist air density ρ_a by using the relation,

$$\rho_a=1.169\times10^{-3}\rho, \tag{55}$$

the expression for the surface stress is

$$n\tau_s=0.0028\rho_a V^2. \tag{56}$$

If the value 1.5 be assigned to n, the value of the surface stress, using the ordinary form of the formula for such stresses, is

$$\tau_s=0.0037\frac{\rho_a V^2}{2}. \tag{57}$$

If it is supposed that the height of the air passage in the present experiments has no effect on the stresses developed on the surface of the liquid, then the shear obtained might be compared with the shear evaluated according to some boundary layer theory applicable to the case of a moving liquid surface. Such a theory is not yet available, and the next best

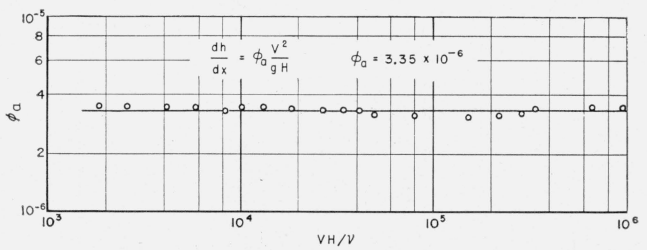

FIGURE 15. *Coefficient of surface slope in the absence of waves as a function of Reynolds Number based on wind velocities.*

choice is therefore to compare our results with the well-known theory of the resistance of smooth plates. In terms of the drag coefficient C_d,

$$\tau_s = C_d \rho_a V^2/2, \tag{58}$$

where

$$C_d = C_d\left(\frac{VL}{\nu_a}\right), \tag{59}$$

and ν_a is the kinematic viscosity of air. In the tests, the results of which are now being examined, the Reynolds number VL/ν_a ranged from 10^6 to 10^7. The drag coefficient for this range as determined by Gebers [5] and by Kempf and Kloess [6] is

$$C_d = 0.0032, \tag{60}$$

and this agrees very well with the corresponding coefficient in eq 57.

It would thus appear that the stress developed over the smooth surface of water under the action of flowing air could be determined with sufficient accuracy by using the ordinary theory of smooth plate resistance.

For emphasis, the foregoing results will be summarized. Shear acting on the liquid surface in the absence of waves is independent of the depth of liquid and the kinematic viscosity of the liquid. The magnitude of the shear is almost identical with the shear that may be associated with the skin friction of smooth plates. In this comparison one may assume that the ratios of the surface shear to the bottom shear is two; that is, $n=1.5$. The value of the ratio is exact in the case of viscous flow; it is not known precisely for the case of turbulent flow. The prevailing flow in the liquid below the surface is determined solely on the basis of the surface velocities, the depth, and the kinematic viscosity of the liquid. For purely viscous flow, the flow is in accordance with the simple one-dimensional theory. The exact conditions and the details of the mechanism of flow in the case of turbulent flow are not known. These could be made the object of a fruitful and a promising special study.

V. Wind Set-Up in the Presence of Waves

1. Effective Air Velocities

In the observations of set-up with smooth water surfaces the variations in the value of the air velocities with distance along the channel axis proved to be small, and they were ignored. On the other hand the corresponding variations were large when the surface of the liquid was covered with waves and due account was taken during the reduction of data. Two causes were operative in producing the variations of the air velocities with distance. First, waves induced comparatively large stresses over the water surface and thus a greater rise in water level in the leeward end of the channel. Second, as the heights of the waves increased with distance, the elevated crests caused a further decrease in the height of the air passage. The air velocity variations with distance were especially marked for the larger depths of water because of the small depth of the channel.

Under these conditions the air velocity values derived from the Venturi nozzle are only nominal velocities, and these had to be modified or corrected to obtain the effective air velocities. The basis of the corrections is as follows:

The local surface gradient at the point x may be written as

$$\frac{dh}{dx} = C\frac{V^2}{gH}, \tag{61}$$

where the coefficient is

$$C = C\left(\frac{x}{L}, \frac{V}{gH}, \frac{H}{L}, \frac{VH}{\nu}\right), \tag{62}$$

which is an assumption of the most general application. If V be constant, the integration of eq 61 yields

$$S = h_2 - h_1 = \frac{V^2}{gH}\int_0^L C\,dx = C_m L\frac{V^2}{gH}. \tag{63}$$

Supposing that V is not constant but $V = V_n + \Delta V$, where ΔV is a small fraction of V_n, the same integration gives

$$S = \frac{V_n^2}{gH}\left[\int_0^L C\,dx + 2\int_0^L C\frac{\Delta V}{V_n}dx\right],$$

or expressed in a different manner

$$S = \frac{V_n^2}{gH}\left[C_m L + 2\eta C_m \int_0^L \frac{\Delta V}{V_n}dx\right], \tag{64}$$

where η is a quantity larger than unity. Comparing with eq 63,

$$V^2 = \left[1 + 2\eta\int_0^L \frac{\Delta V}{V_n}\frac{dx}{L}\right]V_n^2, \tag{65}$$

which gives the effective wind velocity, V, in terms of the nominal wind velocity, V_n. What the exact value of the coefficient η should be is questionable. We have assumed $\eta = 1.5$ as a plausible value for present applications.

To apply the correction to those measurements of set-up that showed considerable restrictions in the air space above the waves it became necessary to observe the variations of $\Delta V/V_n$ along the channel axis for the different depths of water and for the different air velocities. To give an idea of the variations noted, the data for a depth of 11 cm are shown in figure 16. Using these data and also similar data for other depths, the relationship between the effective wind velocity and the nominal velocity was established as shown in figure 17.

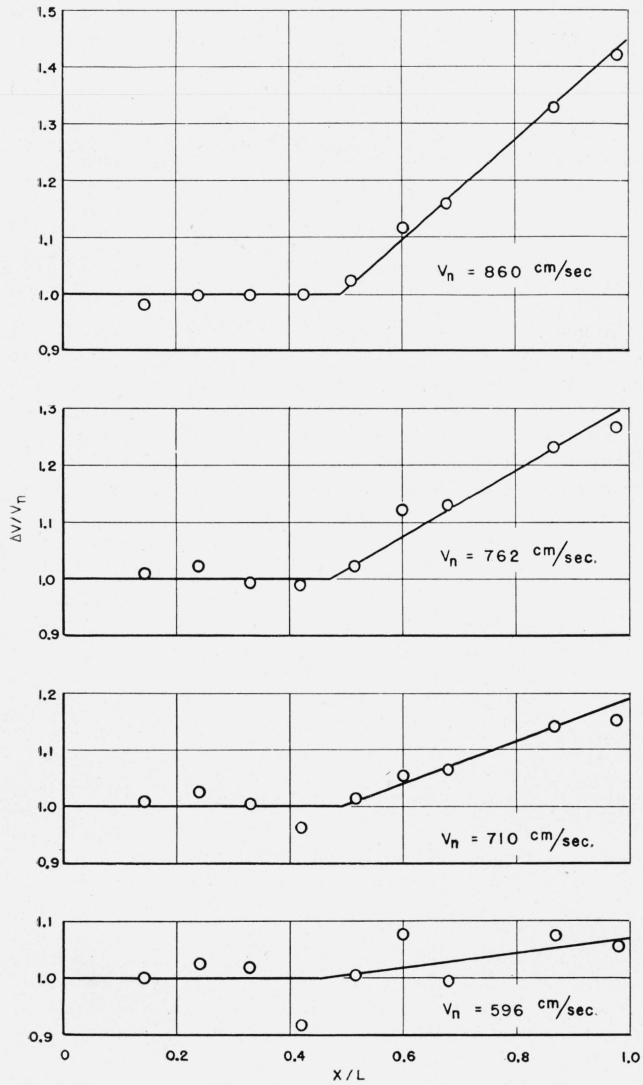

FIGURE 16. *Variation of mean air velocities along the channel axis. Water depth=11.4 cm.*

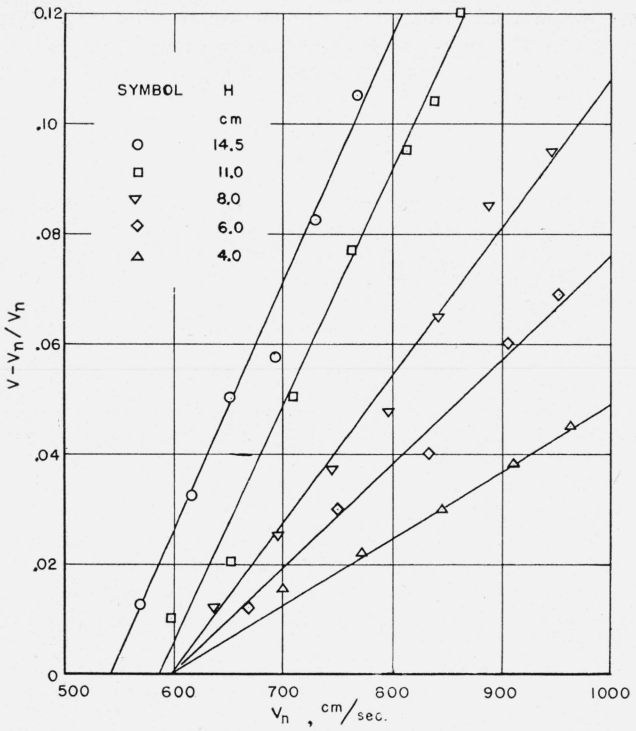

FIGURE 17. *Effective wind velocities in terms of the nominal wind velocities.*

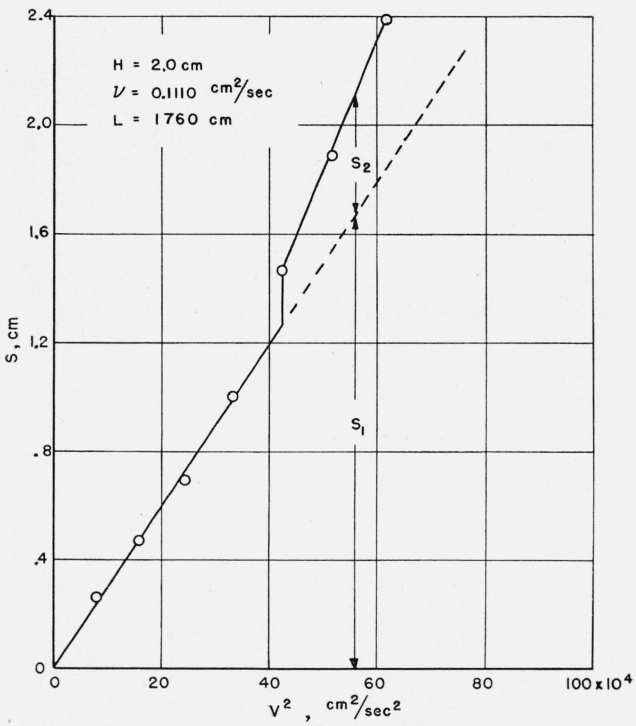

FIGURE 18. *The partitioning of set-up when waves are present.*

2. Dependence of Set-Up on Depth of Water When Waves Are Present

Great difficulty was experienced in the beginning when an attempt was made to establish the relationship between set-up and the depth of water for the case where waves were present. The difficulty was overcome partly by supposing that it is permissible to break the observed set-up into two parts, S_1 and S_2, the first being due to skin friction alone and the second part due to form resistance of the wave crests. It was supposed further that the magnitude of S_1 is not affected by the presence of waves, and indeed that it would be the value that would have been obtained for the prevailing air velocities with a smooth water surface. Thus, if S is the observed total set-up, the part S_2 due to the waves is simply

$$S_2 = S - S_1, \tag{66}$$

where

$$S_1 = 3.30 \times 10^{-6} \frac{V^2}{gH} L. \tag{41a}$$

The latter relationship was fully discussed in the previous sections.

At the moment the dynamical significance of the procedure of partitioning is not clear. The only justification that may be mentioned now is the consistency and the reasonableness of the results obtained. The idea was suggested by the fact that the relationship between the water surface velocities and the wind velocities is not affected by the presence of waves. Eventually, of course, we wish to consider the dynamical aspects of the phenomenon of total resistance in a future investigation. For the present, however, our main interest is in the parametric representation of measured quantities and the validity of these representations for the quantitative evaluations of the set-up.

As an example of partitioning the set-up into parts, the data in figure 18 are presented. The data were obtained with a sugar solution of kinematic viscosity $\nu = 0.111$ cm^2/sec. The surface length was $L = 1760$ cm, and the depth of water was $H = 2$ cm. Due to the high value of viscosity, the surface remained smooth for an appreciably large range of wind velocities, as can be seen from the curve. For this range the set-up varies with the square of the wind velocity as it should. Waves were initiated when the wind velocity exceeded 650 cm/sec. The curve indicates that the increase in the value of the set-up starts with a jump. The projection of the straight line passing through the points of observation corresponding to small wind velocities is indicated by dashes. The quantity S_2 shown in the diagram, which is the excess over the dashed line, is taken to represent that part of the set-up due to waves.

The same method of graphic partitioning was employed in the results of the tests made with water depths of 14.5, 11, 8, 6, and 4 cm. As the tap water used in the tests was relatively pure, waves of substantial size were obtained. The data are given in figures 19 and 20. The straight lines represent the magnitudes of S_1, whereas the curves drawn through

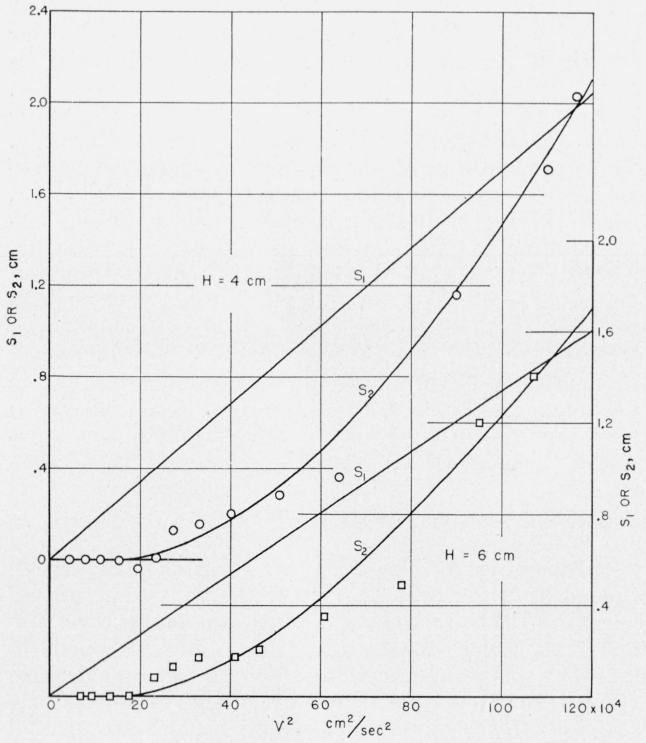

FIGURE 19. *Partial set-up due to waves in tests with small water depths.*

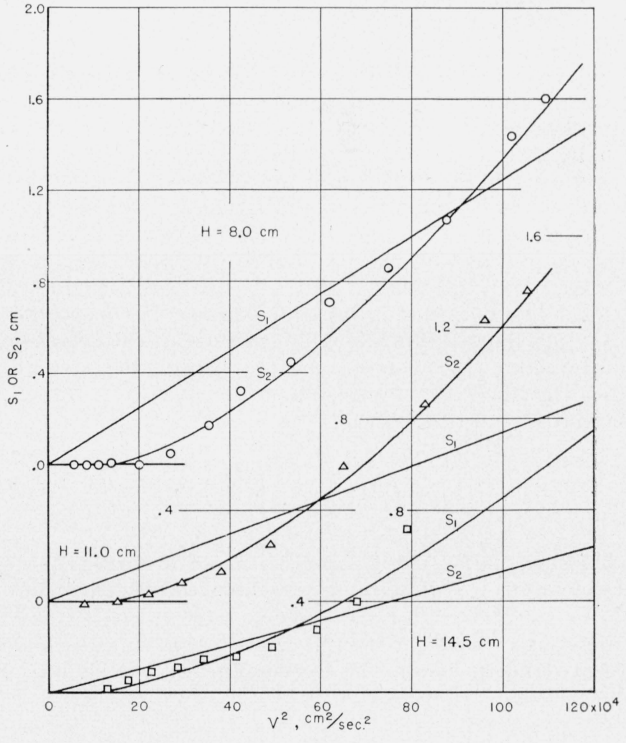

FIGURE 20. *Partial set-up due to waves in tests with large water depths.*

the symbols show the excess of the observed set-up with respect to S_1. These two quantities, S_1 and S_2, are expressed as functions of the squares of the wind velocities. As is seen from the figures, S_2 commences to increase after V has exceeded a certain critical wind velocity, V_0. The figures suggest that the increase starts with a jump. This fact will be ignored, and it will be assumed that the increase is from a null value and the changes are gradual. The curves representing S_2 are drawn accordingly.

On the basis of dimensional reasoning it is to be expected that

$$\frac{S_2}{L}=f_1\left(\frac{V}{\sqrt{gH}},\frac{(g\nu)^{1/3}}{\sqrt{gH}},\frac{\rho}{\rho_a},\frac{H}{L}\right), \tag{67}$$

and as to the identification of V_0,

$$\frac{V_0}{\sqrt{gH}}=f_2\left(\frac{(g\nu)^{1/3}}{\sqrt{gH}},\frac{\rho}{\rho_a},\frac{H}{L}\right). \tag{68}$$

Eliminating the parameter containing the kinematic viscosity,

$$\frac{S_2}{L}=f_3\left(\frac{V}{\sqrt{gH}},\frac{V_0}{\sqrt{gH}},\frac{\rho}{\rho_a},\frac{H}{L}\right). \tag{69}$$

Now, if we take V_0 as 350, 360, 380, 420, and 440 cm/sec, corresponding to water depths of 14.5, 11, 8, 6, and 4 cm, respectively, then the additional set-up S^2 due to the waves may be represented as

$$S_2=C(V-V_0)^2. \tag{70}$$

The evidence for the statement is shown in figure 21. Since in this group of data the quantities L, g, μ are not changed, the factor C may involve the depth H. To determine the nature of dependence on the depth, the values of S_2 corresponding to $(V-V_0)^2=50\times10^4$ are first read from the lines in figure 21 and are then transferred to the logarithmic plot of figure 22. The disposition of the points definitely lacks the even regularity of alinement that one naturally wishes to find. The points may be approximated by a straight line; but there is considerable latitude in the selection of the slope of the line. If one adopts the straight line drawn in the figure, then the equation for the partial set-up due to waves is

$$\frac{S_2}{L}=B\frac{(V-V_0)^2}{gH}\left(\frac{H}{L}\right)^{1/2}, \tag{71}$$

where $B=2.08\times10^{-4}$, and V_0 has the values mentioned above. If we disregard the small variations of V_0 for the different depths, the mean $V_0=390$ cm/sec is a suitable value. Adding to this the part due to skin friction, the expression for the set-up in the presence of waves is

$$\frac{S}{L}=A\frac{V^2}{gH}+B\frac{(V-V_0)^2}{gH}\left(\frac{H}{L}\right)^{1/2}, \tag{72}$$

where

$$A=33.0\times10^{-6}, \qquad B=2{,}08\times10^{-4},$$

It is understandable that the expression represents with sufficient accuracy the data that were observed. Yet, neither the reality nor the dynamical significance of the quantity V_0 appearing in the formula can be discussed at the moment in a manner satisfactory to us. For this reason the quantity V_0 will be referred to as the formula characteristic velocity.

3. Effect of Viscosity on Partial Set-Up Due To Waves

It was shown previously, working with the data for smooth water surfaces, that the partial set-up S_1 is independent of viscosity. It now remains to investigate what effect, if any, viscosity will have on the partial set-up due to waves, that is on S_2.

To consider this matter, a series of tests was carried out with a constant liquid depth of 8 cm. In addition to water, sugar solutions of four different concentrations were used, thus making altogether five experimental liquids of unequal kinematic viscosities. The setups observed with these liquids for an effective surface length of 1,900 cm are shown in figure 23. The two components, S_1 and S_2, of the total setup are plotted as functions of the squares of the wind velocities. It is to be noted that the S_1 line is common to all the liquids and is independent of viscosity. After drawing the curves through the S_2 points of observation, values of S_2 were read from these curves, the square roots of which are plotted in figure 24 against the wind velocity. The disposition of the points is linear. This would mean that the form of the expression in eq 70 is valid for liquids of varying viscosity. The lines have practically the same inclination independent of viscosity, and thus the value of C in eq 70, and hence the value of B appearing in eq 71, is not affected by viscosity. The intersections of the lines with the axis of velocities give the formula characteristic velocity, V_0, which varies with the viscosity. Specifically, corresponding to the successive viscosities $\mu=0.0092$, 0.0154, 0.0217, 0.0351, 0.0600 cm^2/sec, the formula velocities are $V_0=380$, 630, 680, 720, 900 cm/sec, respectively.

Summarizing, the only effect of the increased viscosities is to increase the formula characteristic velocity. As a result, then, the total setup observed for a given wind velocity decreases when the kinematic viscosity of the liquid is increased.

4. An Analysis of Hellström's Data on Setup

In deriving the law of setup expressed by eq 72, the assumption was made tacitly that the limited height of the air passage over the surface of the water in these experiments does not substantially modify the magnitude of the resulting setups. Had it not been for the fixed construction of the channel, this circumstance would have been studied experimentally by varying the height of the air passage for a given depth of water. Fortunately

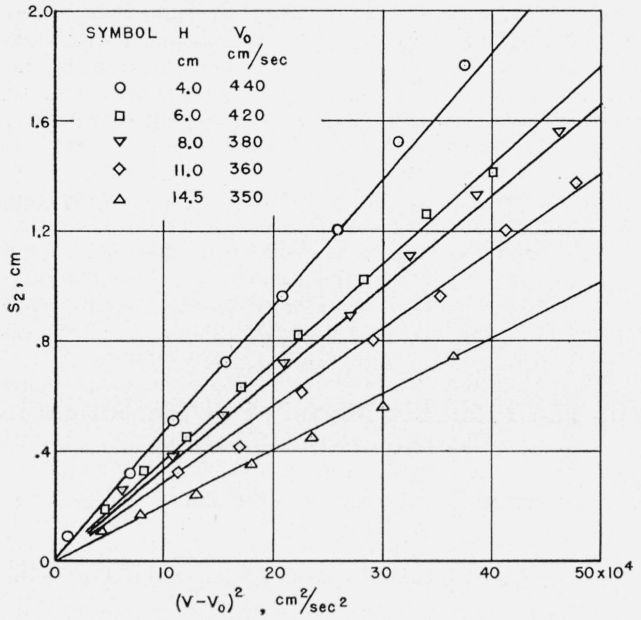

FIGURE 21. *The relation of the formula characteristic velocity to the partial set-up due to waves.*

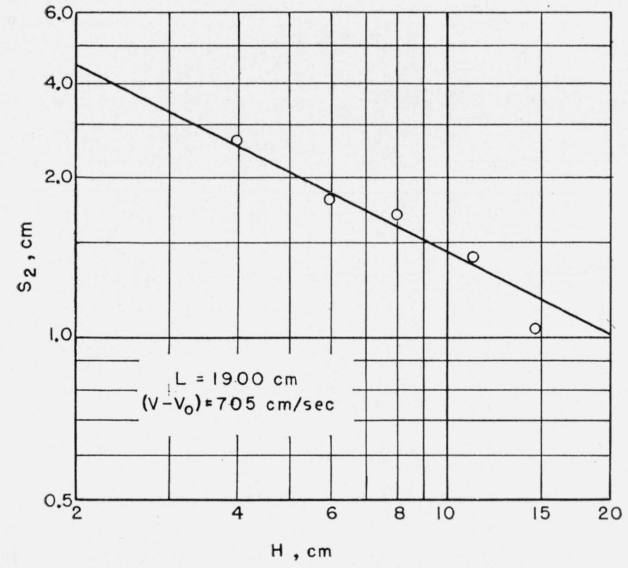

FIGURE 22. *Effect of depth on partial set-up due to waves.*

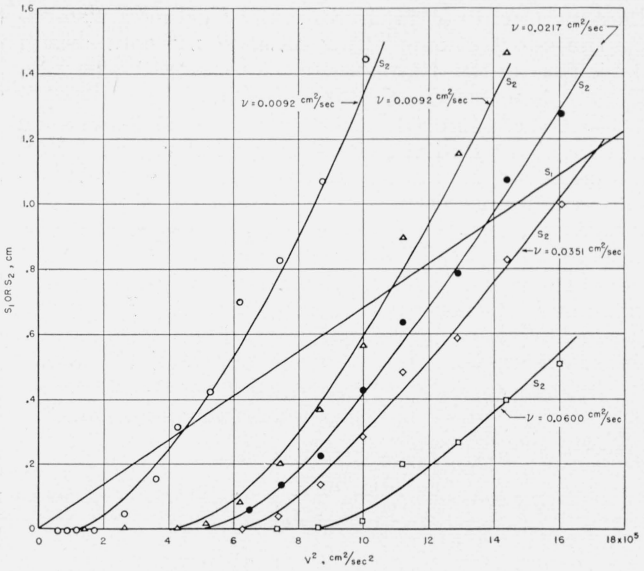

FIGURE 23. *Effect of viscosity on partial set-up due to waves.*

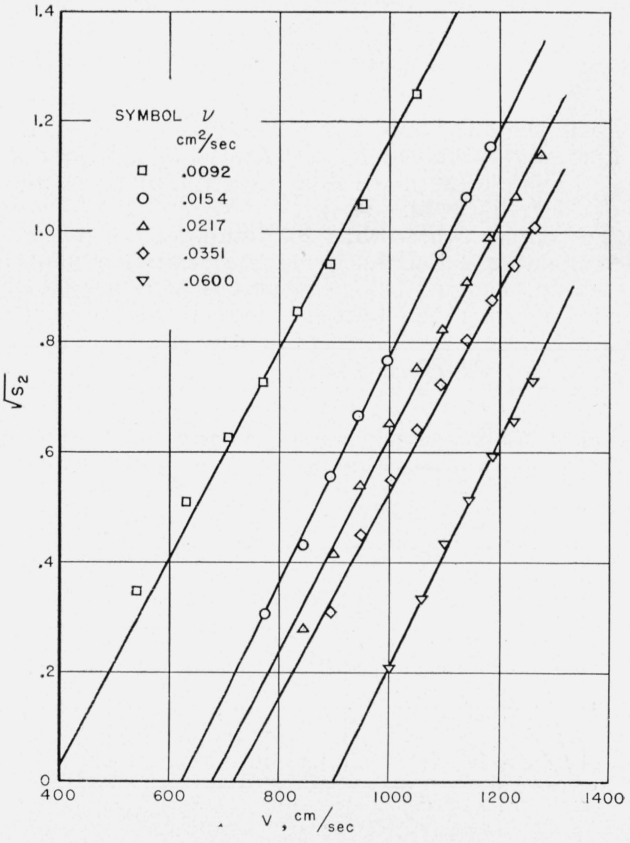

FIGURE 24. *The determination of formula characteristic velocities.*

the experiments of Hellström are of value in discussing the effect of size of air passage by comparison of results, as the channel used by Hellström had an air passage of relatively large depth.

The data in figure 25 give the relationship between surface shear and depth of water for various wind velocities as found by Hellström. One modification was made on our part; that is, to conform to our results channel central velocities were changed to mean velocities in the channel cross section. The data in this figure may be made the basis on which to deduce the set-up magnitudes in the Hellström channel. The channel had a length of 300 cm and a depth of 50 cm. The average depth of the water in the experiments appeared to have been varied between the limits of approximately 2 and 4 cm.

From the relation

$$\frac{dh}{dx}=\frac{n\tau_s}{\rho gH}, \tag{22b}$$

if the set-up is small, can be derived the expression

$$S=\frac{n\tau_s L}{\rho gH}, \tag{73}$$

which connects the set-up with the effective average wind force over the entire fetch. Since Hellström has assigned to n the value 1.50, the proper relation to be used in deducing the set-up in his experiments is

$$S=\frac{1.5\,\tau_s L}{\rho gH}. \tag{74}$$

Taking the data from figure 25, sequences of set-up values were obtained for the depths of 2, 3, and 4 cm. These computed values are given by the points plotted in figure 26.

To compare these with the results of the present investigation it suffices to determine similar values of set-up, using eq 72. Now, it will be remembered that for water the formula characteristic velocity showed slight variations from the mean, $V_0=390$ cm/sec, as the water depths where changed. We wish to assign a similar tendency to be valid in the Hellström tests. Accordingly we assign to V_0 the magnitudes 410, 390, and 370 cm/sec to apply to the depths of 2, 3, and 4 cm, respectively. The computed values of the set-ups on this basis, using our general formula, are shown likewise in figure 26. The curves of the computed set-up values form a band, and the Hellström values are within this band. Moreover, the sequence of the curves is the same as the sequence of the Hellström set-up values as the depths are changed. This shows that there is quite a satisfactory agreement between the general formula and the results from the Hellström channel. Accordingly, we are permitted to infer that the restrictive effect of the small air passage in our experiments, if present, must have been small indeed.

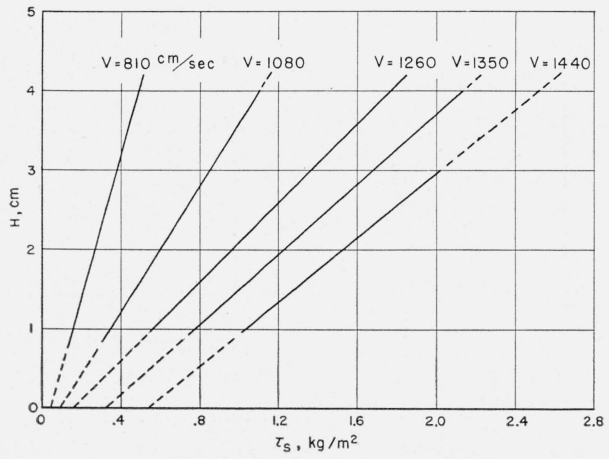

FIGURE 25. *The relation between wind velocity and depth of water in Hellström's experiments.*

VII. The Probable Meaning of the Formula Characteristic Velocity

1. Dimensional Requirements of the Monomial Set-Up Formulas

Before we consider various topics related to the question of the formula characteristic velocities, it becomes necessary to see if the total set-up in association with waves can admit representation by a single term. The general formula developed in this investigation is at variance with this possibility, whereas a monomial formula is implied in the work of Hellström.

Hellström proposes that the relation between the wind force and the wind velocity be of the form

$$\tau_s \sim HV^3. \tag{75}$$

In view of the relation

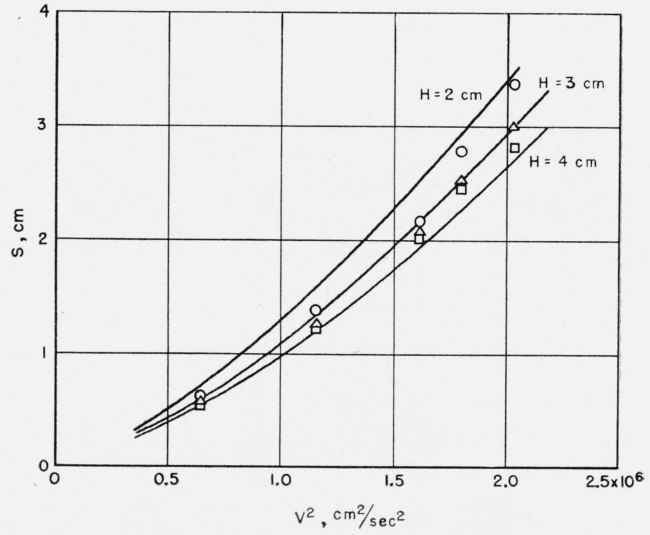

FIGURE 26. *Comparison of set-ups from the Hellström experiments with values obtained from equation 72.*

$$\frac{dh}{dx}=\frac{n\tau_s}{\rho gH}, \tag{22c}$$

one must now infer that the corresponding expression for set-up is

$$\frac{S}{L}=A'V^3, \tag{76}$$

where A' is independent of the depth of water.

The set-up values that were deduced previously and considered during the analysis of the Hellström data are reproduced in figure 27. There are reproduced also the set-up values observed in the tests of the present investigation with water for the region of high wind velocities. The graph representation is logarithmic and the observation points of the two groups of tests, one from Hellström's channel which was 300 cm long and the other from our channel, which was 1,900 cm long, aline themselves linearly. In both cases the inclination of the lines representing the points may be taken to be approximately 3 to 1. Thus the formula of eq 76, applies equally well to the two groups of data from water surfaces covered with waves.

Now in order that eq 76 may represent the physical law of set-up in laboratory channels, the right-hand member must be a dimensionless expression since the left-hand member is a dimensionless ratio. It will

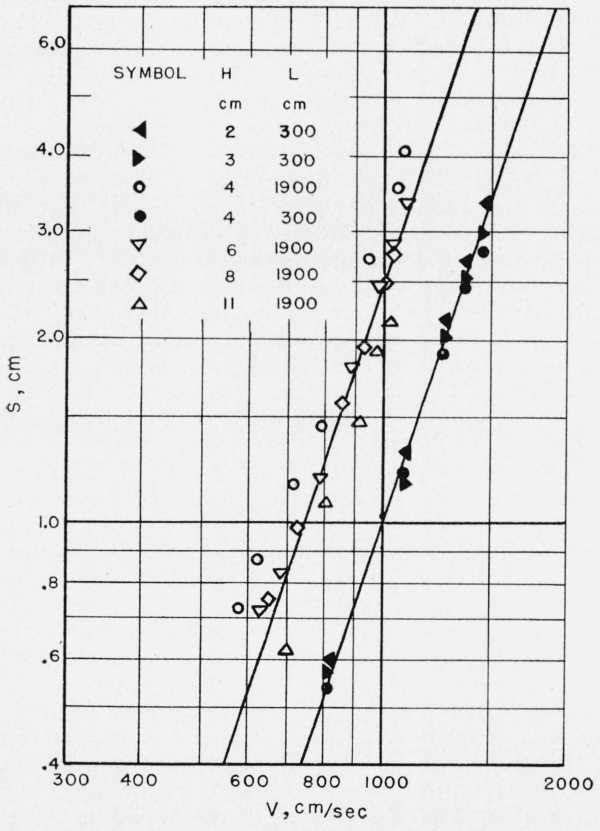

FIGURE 27. *Monomial formula of set-up with waves.*
ν=0.009 to 0.010 cm²/sec.

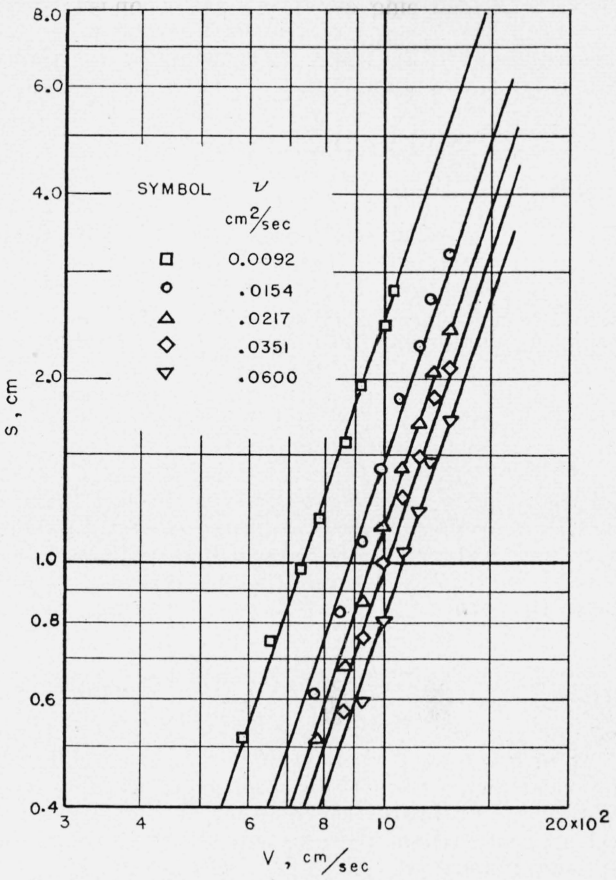

FIGURE 28. *Monomial formula for variable viscosities.*
L=1900 cm. H=8.0 cm.

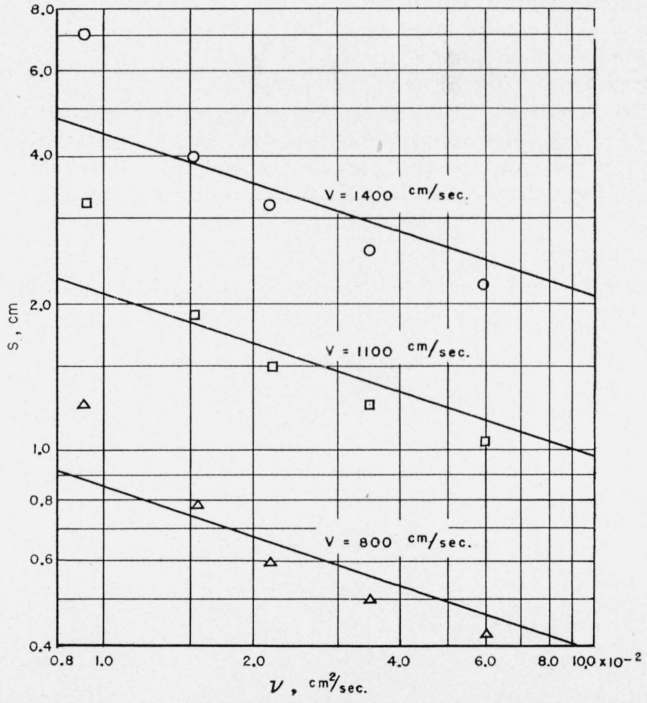

FIGURE 29. *Monomial formula of set-up formulating the effect of velocity.*

be remembered that the data now being considered are from two groups of tests where the kinematic viscosities were the same. Accordingly, the general law could be

$$\frac{S}{L}=A'\left(\frac{V}{\sqrt{gL}}\right)^3 f\left(\frac{\sqrt{gL}L}{\nu}\right). \tag{77}$$

The right member contains a factor involving the kinematic viscosity. The influence of this factor may be determined by considering the set-up data obtained with highly viscous sugar solutions subjected to large wind velocities. These data are shown in a separate logarithmic plotting in figure 28. The distribution of the points for a given viscosity are linear, and furthermore the inclination of the lines are in agreement with the expression in eq 77.

If the S values for the velocities V=1,400, 1,000, and 800 cm/sec be considered, as in figure 29, it is seen that these may be approximated by straight lines with a slope of $-\frac{1}{3}$. Accordingly, if the expression in eq 76 does represent a physical law, it must be of the form

$$\frac{S}{L}=A'\left(\frac{V}{\sqrt{gL}}\right)^3\left(\frac{\sqrt{gL}L}{\nu}\right)^{1/3}. \tag{78}$$

It now remains to be seen if this is actually the physical law for the set-ups observed in the laboratory channels. Owing to the manner of the derivation, the separate exponents represent the effects of velocity and kinematic viscosity. To examine the contingency that these exponents represent likewise the effect of channel length, the last expression will be written in the form

$$S=A'\frac{V^3}{g^{4/3}\nu^{1/3}}. \tag{79}$$

Accordingly, wind velocities and kinematic viscosities remaining the same, the set-up observed is independent of the length of channel. As this deduction is contrary to observation, it is to be inferred that the monomial form for expressing the set-up is invalid when set-ups are observed in laboratory channels with the wind velocities sufficiently high to produce waves.

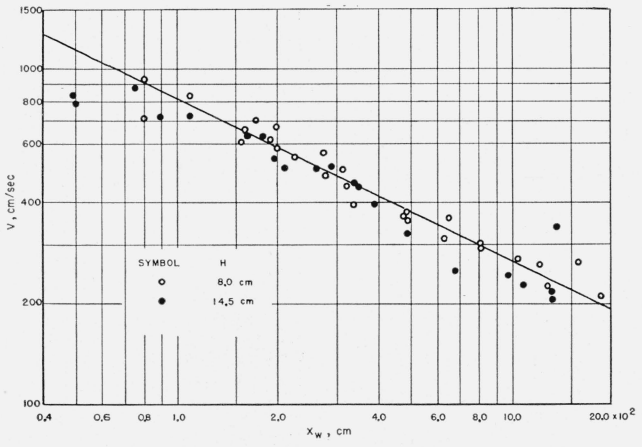

FIGURE 30. *Variation of initial fetch for the start of waves with wind velocity.*

2. Critical Wind Velocity for Wave Formation

It was noted during the preparation of data for analysis that almost invariably the formula characteristic velocity exceeded the critical wind velocity for generating waves. It may prove to be of some significance if a relationship can be established between these two velocities. This in turn requires that the law giving the critical wind velocity for wave formation be first established.

At very low wind velocities the surface of the water remained calm. In fact if one studied the images of the vertical and the horizontal bars of windows reflected from the water surface, they appeared as even bands extending laterally and longitudinally over the water surface. On increasing the wind velocity, a tremor of the water surface was noticed, and the reflections of the bars now had the appearance of sinusoidal bands. This condition extended from one end of the channel to the other, except that there was a tendency for the amplitudes of the irregularities to increase somewhat with distance. With a further increase of the wind velocity the tremor of the water surface was considerably augmented until finally the reflected shadows were confused. Experience showed that this state of the water surface was precedent to the appearance of waves, and in fact only a slight further increase in the wind velocity would be sufficient for the formation of waves.

The waves first formed were two dimensional, their length being estimated to be close to 4 cm. The wave heights were less than 2 mm, but this value could not be definitely determined since it was effected by the meniscus at the glass wall. Initially when the waves were formed, they did not cover the entire area of the water surface but were seen first in the leeward part of the channel. This would mean that an initial fetch of length, X_w, is necessary for the waves to appear, or more precisely to be visible to the eye. With increasing wind velocities the length of the initial fetch gradually decreased. To examine the magnitude of the decrease a few observations were made at water depths of 14.5 and 8 cm. The data from these observations are shown in figure 30. It is obvious that for these observations the initial fetch is inversely proportional to the square root of the velocity of the wind. When the initial fetch decreased to a length of about 1 or 1½ m, a new condition of the surface was manifested. The area between the windward water edge and the locality where the initial two-dimensional waves of the wavelength of 4 cm were first noted was covered with ripples. These ripples were three-dimensional and were about 2 cm long. One noticed with amazement the sharp and distinct issuing of the initial two-dimensional waves of wavelength of 4 cm at the lower end of the area of the ripples. With

greater wind velocities the initial area of the ripples was somewhat decreased; but in these investigations the length of the area never fell below 60 cm.

When the initial fetch for the startof the waves was small, which occurred at high wind velocities, wave height and wavelength increased with distance. With some exceptions, the increase of the wave height was proportional to the square root of distance, whereas the increase of wavelength was proportional to the distance. When the initial fetch was large, which corresponded to small velocities, it was observed at times that the waves once formed would be damped out, but reappeared near the leeward end of the channel.

The condition of variable fetch at the start of the waves and the tendency of waves to damp out when the wind velocity was small made it difficult to determine the particular wind velocity to be associated with the formation of waves. The matter of observation of the critical wind velocities for wave genesis was resolved as follows. Three initial fetches, of lengths 1,000, 800, and 600 cm were selected and the corresponding wind velocities determined. The average value of the three velocities was taken to represent the critical wind velocity, V_c, for the wave formation. When using water alone, the critical wind velocities were determined for depths of 14.5, 11, 8, 6, and 4 cm. When using more viscous solutions, the depths were 8, 4, and 2 cm.

In the presentation of data we follow the procedure of dimensional analysis. If it be assumed that the critical wind velocity is independent of fetch, then the dependence can be on the depth of water, the kinematic viscosity of the liquid, and the densities of the air and the liquid. Accordingly,

$$\frac{V_c}{\sqrt{gH}} = f([g\nu\rho/\rho_a]^{1/3}/\sqrt{gH}). \tag{80}$$

Conforming with this, the observed data are presented in the logarithmic plotting in figure 31. Despite the difficulty encountered in the observation of the critical wind velocities, the distribution of the points is sufficiently regular to allow the drawing of a straight line to represent them. Since the slope of the line drawn is unity, the critical wind velocity is independent of depth of liquid. Accordingly the desired form of the law is, very simply,

$$V_c = 16.2(g\rho\nu/\rho_a)^{1/3}. \tag{81}$$

Interestingly enough the form of the criterion accords well with the form that Harold Jeffreys [7] has derived theoretically. The only disagreement is in the numerical values of observation. The observations made by Jeffreys in open lakes and rivers suggest that the numerical value of the coefficient is about one-third as great as that given in eq 81. The cause of the disagreement may be the possibility that the critical value in reality depends also on the fetch of the initial waves noted. This aspect of the question deserves an examination in channels of variable lengths.

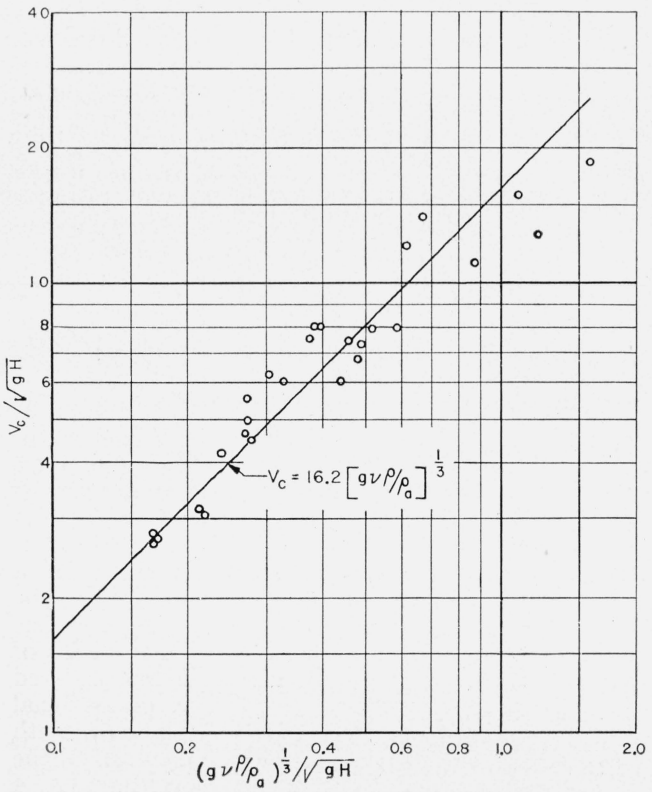

FIGURE 31. *Critical wind velocity for the start of waves.*

3. Correlation Between the Critical Wind Velocity and the Formula Characteristic velocity

As mentioned previously, it was noted during the work of data reduction that a correlation may exist between the critical wind velocity and the formula characteristic velocity. Since, as shown above, the factors affecting the critical wind velocity assume a very simple relationship, it would likewise seem sufficient to consider the dependence of the formula characteristic velocity on the kinematic viscosity and the channel length in the manner carried out in figure 32. The open circles in the figure are the values obtained during the analysis of the set-up due to waves, and the values of the associated formula characteristic velocity were indicated previously. The values corresponding to the black

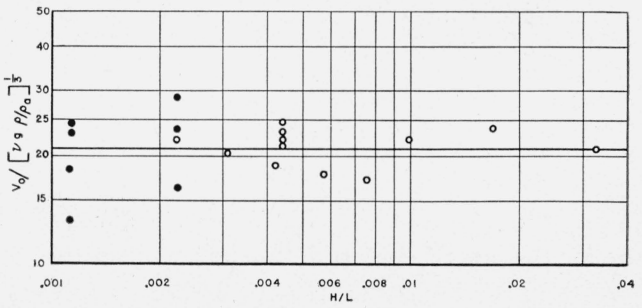

FIGURE 32. *Variation of the formula characteristic velocity with viscosity.*

circles were obtained in a different manner. The method is suggested from the graph in figure 18. The velocity concurrent with the sudden increase in the set-up values due to the presence of waves is interpreted as a value close to V_0. The full circles are from tests with small liquid depths and with high viscosities.

The distribution of the points suggests that it should suffice to represent the data by a horizontal line. Thus the formula characteristic velocity is independent of channel length and is proportional to critical wind velocity for the generation of waves. More specifically

$$V_0=21.0(g\rho\nu/\rho_a)^{1/3}. \tag{82}$$

The reader unquestionably will suspect, and this very justly, that we have tended to an over-simplification in this representation. Although the use of the formula characteristic velocity has caused a simpler representation of the set-up relationship in the general formula, this velocity by itself must have reference to various hydrodynamic elements involving dissipation and relative velocities such as the velocity of the waves with respect to the velocity of wind and also the velocity of the drift current at the surface of the water. At the moment the author is not prepared to discuss these matters satisfactorily. If dissipation really plays a large part in forming the formula characteristic velocity, then the opinion may be expressed that with greater liquid depths the magnitude of the formula characteristic velocity decreases.

4. A Possible Mathematical Basis for the Law of Partial Set-up Due To Waves

As mentioned before, between the points representing S_2 values and the curves intended to represent the course of the data, there exist small disparities. This fact no doubt has a bearing on the accuracy of the determinations, first of the formula velocity, V_0, and second of the exponent of H/L occurring in the formula for the partial set-up S_2, that is in the expression of eq 71. Accordingly, if one can formulate a mathematical basis that will justify the form of the law for S_2, independent of the actual methods of reductions used, this should prove to be very illuminating.

Pursuant to our original ideas and opinions we will suppose that when waves are present each crest contributes an additional resistance, and the resistance, in its major part at least, is due to form resistance. Let R be the resistance. The length of waves being λ, the added shear due to waves is

$$\tau_{s2}=R/\lambda. \tag{83}$$

As for the law relating to R we may suppose that

$$R=c\rho_a(V-V_0)^2a, \tag{84}$$

where a is the half value of wave height. At the moment nothing will be said as to the cause or the origin of V_0. Thus, the added shear is

$$\tau_{s2}=c\rho_a(V-V_0)^2a/\lambda. \tag{85}$$

Substituting in the expression

$$\left(\frac{dh}{dx}\right)_2=\frac{\tau_{s2}}{\rho gH}, \tag{22c}$$

and integrating with respect to x, there is obtained

$$S_2=c_1\frac{(V-V_0)^2}{gH}\int_0^L\frac{a}{\lambda}\,dx. \tag{86}$$

If the variation of a/λ with respect to x be known for the waves generated in shallow channels by the action of wind, the integration required above will lead to an expression for the set-up S_2 due to waves only.

Next it shall be supposed that the law of growth of waves in shallow waters is virtually

$$a\sim V^{1/2}Hx^{1/2}, \tag{87}$$

and

$$\lambda\sim V^{1/2}H^{1/2}x, \tag{88}$$

for sufficiently large values of V. Hence, we have

$$\frac{a}{\lambda}=c_2\left(\frac{H}{x}\right)^{1/2}. \tag{89}$$

That is, the steepness of wind waves in shallow water decreases with distance in the leeward direction. Since

$$\int_0^L\frac{a}{\lambda}\,dx=c_3H^{1/2}L^{1/2}, \tag{90}$$

there results, by substituting in eq 86

$$\frac{S_2}{L}=B\frac{(V-V_0)^2}{gH}\left(\frac{H}{L}\right)^{1/2}, \tag{91}$$

which in fact is the form that was adopted in the analysis of the set-up due to waves.

In the above derivation three separate assumptions are used. These are represented by eq 85, 87, and 88. Each of these assumptions is amenable to experimental examination. This work is now under way.

VIII. An Application to Natural Conditions

In his fine treatise Hellström gives some data on the wind effects of storms on Lake Erie. It will be interesting to compare the magnitudes of the set-ups occurring during these storms with the computed values to be obtained with the general formula of the present investigation. The observed set-ups at Lake Erie are shown in figure 33 by the plotted points.

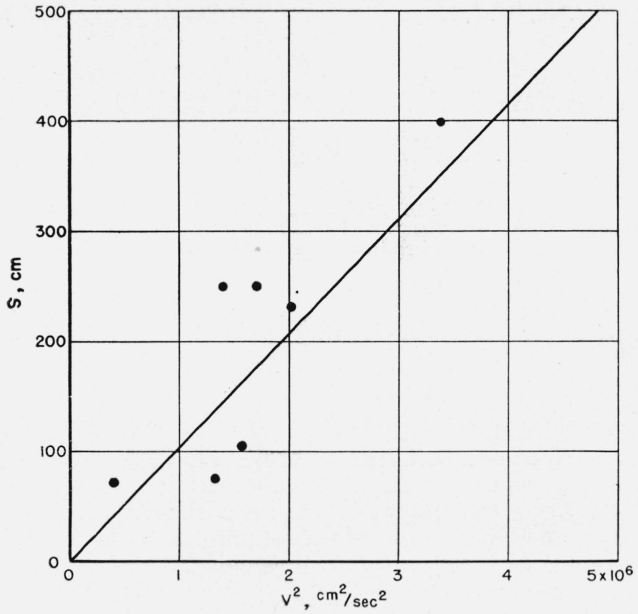

FIGURE 33. *Comparison of observed set-up in Lake Erie during storms with equation 87.*

In applying the general formula, eq 72, a statement is necessary regarding the value of the formula characteristic velocity appropriate for natural conditions. As was mentioned previously, the critical wind velocity for the genesis of waves on large bodies of water is about one-third as great as the corresponding value obtained in our laboratory channel. Furthermore, it was also shown that the formula characteristic velocity is about 1.3 times larger than the critical wind velocity. Thus it is to be expected, as the formula characteristic velocity is of the order of 100 cm/sec for large bodies of water, that only a minor error will be made if this velocity is omitted. With this understanding the set-up expression for natural conditions may be given in the form

$$\frac{S}{L}=3.30\times10^{-6}\left[1+63\left(\frac{H}{L}\right)^{1/2}\right]\frac{V^2}{gH}, \qquad (87)$$

and this should apply to large bodies of water, the confinement approximating the shape of a rectangular channel of a uniform cross section.

The average depth of Lake Erie being 17.7 m and the length 377 km, computations on the basis of the above formula gave a set of values of the expected set-up shown by the heavy straight line in figure 33. It will be remembered that the difference between the surface elevations at the extreme ends of the lake is defined as the set-up.

The agreement between the laboratory results and the observed set-up during storms may be deemed satisfactory. However, this relationship can neither be elaborated on nor discussed with a sense of finality. In order to make a definite evaluation of the rigor of the general formula proposed on the basis of the tests of the present investigation, it is necessary to have reliable observational data from numerous lakes or reservoirs with different depth/length ratios. Such data are not known to us at the present.

IX. The Need of New Experiments

One of the most significant deductions from the general set-up formula developed from these tests is in relation to the effective stresses at the surface of the water. Ordinarily it is supposed that the stress or the wind force is independent of the length of channel. The tests of the present investigation, however, show that the stress depends on the length of the channel. If this result holds in general, model experimentation on wind effects to simulate prototype conditions and effects will be out of the question.

Regarding this effect of channel length, two possibilities may be imagined. First, the effect of the length on the effective magnitude of the wind force may continue indefinitely when the channel length is increased keeping the water depth constant. Second, the effect may become gradually less important with increased length and less than that required by the general formula now given.

These matters can be studied within certain limitations in a new series of tests with channels much longer than the channel used in the present investigation. At the National Hydraulic Laboratory there are now available channels of sufficient length, and it is our intention to resume experiments when opportunity permits.

The author expresses his appreciation for the careful and thorough experimental work of his assistants, Marion R. Brockman and Victor Brame, without which it would have been impossible to complete this investigation.

X. References

[1] H. U. Sverdrup and W. H. Munk, Wind, sea and swell: Theory of relations for forecasting, Hydrographic Office, United States Navy Department, H. O. Pub. No. 601 (March 1947).

[2] B. Hellström, Wind effects on lakes and rivers, Handlingar, Ingeniörs Vetenskaps Akademien; Nr. 158 (Stockholm, 1941).

[3] G. B. Schubauer and M. A. Mason, Performance characteristics of water current meters in water and in air, J. Research NBS **18,** 351 (1937) RP981.

[4] U. Roll, Das Windfeld über den Meerswellen, Naturwissenschaften **35,** 230 (1948).

[5] Gebers, Das Ähnlichkeitsgesetz für den Flächenwiderstand im Wasser geradlinig fortbewegter, politierter Platten, Schiffbau **22,** 687 (1919).

[6] Kempf und Kloess, Widerstand kurzer Flächen, Werft, Reederei, Hafen **6,** 435 (1925).

[7] H. Jeffreys, Formation of water waves by wind, Proc. Roy. Soc. [A] **110,** 241 (1926).

WASHINGTON, November 3, 1950.